Electronic Supplementary Information (ESI)

SecScan: a general approach for mapping disulfide bonds in synthetic and recombinant peptides and proteins

Stepan S. Denisov[a], Johannes H. Ippel[a], Ben J. Mans[b, c], Ingrid Dijkgraaf[†a], and Tilman M. Hackeng[†*a]

[a] Department of Biochemistry, University of Maastricht, Cardiovascular Research Institute Maastricht (CARIM, Universiteitssingel 50, 6229 ER, Maastricht (The Netherlands)

[b] Epidemiology, Parasites and Vectors, Agricultural Research Council-Onderstepoort Veterinary Institute, Onderstepoort 0110, South Africa

[c] Department of Life and Consumer Sciences, University of South Africa, South Africa

† I. Dijkgraaf and T.M. Hackeng contributed equally to the manuscript

* Corresponding author: t.hackeng@maastrichtuniversity.nl

Table of content

Materials and methods 3
Fig. S1. NMR analysis of Arg-vasopressin Sec1/Sec6 9
Fig. S2. LC-MS analysis of purified Arg-vasopressin variants. 10
Fig. S3. Chemical shift perturbations induced by Se in C1U/C6U Arg-vasopressin. 11
Fig. S4. Chemical shift perturbations induced by Se in C6U Arg-vasopressin. 12
Fig. S5. LC-MS analysis of purified μ-conotoxin KIIIA variants. 13
Fig. S6. Chemical shift perturbations induced by Se in C1U μ-conotoxin KIIIA. 14
Fig. S7. Chemical shift perturbations induced by Se in C2U μ-conotoxin KIIIA. 15
Fig. S8. Chemical shift perturbations induced by Se in C4U μ-conotoxin KIIIA. 16
Fig. S9. LC-MS analysis of purified Kalata B1 variants. 17
Fig. S10. Folding kinetics of wt Kalata B1. 18
Figure S11. Folding kinetics of C5U Kalata B1. 19
Figure S12. Folding kinetics of C22U Kalata B1. 20
Figure S13. Folding kinetics of C27U Kalata B1. 21
Figure S14. Folding kinetics of C29U Kalata B1. 22
Figure S15. Chemical shift perturbations induced by Se in C27U Kalata B1. 23
Figure S16. Chemical shift perturbations induced by Se in C5U Kalata B1. 24
Figure S17. Chemical shift perturbations induced by Se in C29U Kalata B1. 25
Figure S18. Chemical shift perturbations induced by Se in C22U Kalata B1. 26
Figure S19. LC-MS analysis of purified BPTI variants. 27
Figure S19. HPLC chromatograms of BPTI variants folding progression recorded at different time points. 28
Figure S20. Chemical shift perturbations induced by Se in C14U BPTI. 29
Figure S21. Chemical shift perturbations induced by Se in C30U BPTI. 30
Figure S22. Chemical shift perturbations induced by Se in C5U BPTI. 31
Figure S23. LC-MS analysis of purified tEv3 (17-56) variants 32
Figure S24. Folding kinetics of C26U tEv3 (17-56) 33
Figure S25. Folding kinetics of C33U tEv3 (17-56) 34
Figure S26. Chemical shift perturbations induced by Se in C22U tEv3 (17-56). 35
Figure S27. Chemical shift perturbations induced by Se in C26U tEv3 (17-56). 36
Figure S28. Chemical shift perturbations induced by Se in C33U tEv3 (17-56). 37
Figure S29. LC-MS analysis of purified BSAP1 variants. 38
Figure S30. Chemical shift perturbations induced by Se in C18U and C22U BSAP1. 39
Table S1. Sequences of synthetic peptides and proteins 40
Table S2. Sequences of BSAP1 variants genes 42
Table S3. Summary table of calculated and observed by ESI-MS masses for all peptides and proteins. 44
Table S4. Summary table of chemical shift differences for Cα/Cβ cysteine atoms. 45

Materials and methods

Peptide synthesis.

Peptides were synthesized manually by regular Boc-SPPS synthesis on Pam or MBHA resin (Table S1). In short, each cycle consisted of a deprotection step by two 1 minute TFA treatments, addition of a pre-activated amino acid followed by DMF washing. Boc-protected amino acids (4-fold excess to a resin) were activated by equimolar amount of HCTU and three-fold molar excess of DIPEA. Coupling of Gln residues included additional washing step by DCM to avoid heating and subsequent intramolecular pyrrolidone formation. Deprotection of Xan-protected residues was carried out in the presence of 5% TIS to prevent a reaction of the xantyl group with Trp residues.

After completion of a peptide chain, peptides were deprotected and cleaved from resin by anhydrous HF treatment for 1 hour at 0°C in the presence of 4% p-cresol as a scavenger. Crude peptides then were precipitated by ice-cold ether, dissolved in 50% aqueous acetonitrile with 0.1% TFA and lyophilized.

Oxidation of Arg-Vasopressin.

To oxidize Arg-Vasopressin, 20 mg of crude peptides were dissolved at RT in 1M Gdn-HCl, 0.1M Tris, 1% H_2O_2, pH 8 to a final concentration of 1 mg/ml. The oxidation was followed by LC-MS. Typically, the reaction was completed after 1 hour, and the peptides were then purified using HPLC. C1U/C6U Arg-Vasopressin was purified without the oxidation step, because of rapid, spontaneous oxidation of selenocysteines. Yield: 2-3 mg.

Cyclization and oxidative folding of Kalata B1.

The one-pot cyclization and oxidative folding procedure was adopted from [1]. 20 mg of crude peptides were dissolved in a minimal volume of 6M Gdn-HCl, 0.1M Tris, pH 8 and then diluted by 1M Gdn-HCl, 0.1M Tris, pH 8 to a final concentration of 1 mg/ml. The mixture was stirred at RT and analysed by LC-MS. Folded Kalata B1 variants were purified by HPLC using a 22mm x 250mm Vydac C18 column, analysed by LC-MS and lyophilised. Yields 1-1.5 mg.

Oxidative folding of truncated Evasin-3

50 mg of crude peptides were dissolved in a minimal volume of 6M Gdn-HCl, 0.1M Tris, pH 8 and then diluted by 1M Gdn-HCl, 0.1M Tris, 10 mM cysteine, 1 mM cystine, pH 8 to a final crude peptide concentration of 1 mg/ml. The mixture was stirred at 4 °C and analysed by LC-MS. Folded truncated Evasin-3 variants were purified by HPLC using a 22mm x 250mm Vydac C18 column, analysed by LC-MS and lyophilised. Yield: 2-3 mg.

Oxidative folding of µ-conotoxin KIIIA

To obtain folded µ-conotoxin KIIIA a polymer-supported oxidation approach was implemented. 100 mg of CLEAR-OX™ resin (Peptides International, 0.27 meq/g) was allowed to swell in DCM for 30 min, followed by a washing step with 50%/50% DCM/MeOH and 1M Gdn-HCl in 0.1M MES buffer pH 6. Next, 50 mg of crude µ-conotoxin KIIIA variants were dissolved in 1M Gdn-

HCl, 0.1M MES, pH 6 to a final concentration of 5 mg/ml and folded in presence of the CLEAR-OX™ resin. The mixture was stirred overnight at RT. Folded KIIIA variants were purified by HPLC using a 10mm x 250mm Vydac C18 column, analysed by LC-MS and lyophilised. Yield: 1 mg.

Native chemical ligation of BPTI.

C-terminus and N-terminus BPTI fragments were mixed at a concentration of 10 mg/mL each, in 0.1M Tris-HCl, 6M Gdn-HCl, 2% (v/v) thiophenol, 2% (v/v) benzyl mercaptan, pH 8. The solution was left to react for 5 hours at 37 °C, and intermittently mixed every 30 minutes. Ligated material was purified by HPLC using a 22mm x 250mm Vydac C18 column, analysed by LC-MS and lyophilised.

Oxidative folding of BPTI.

The BPTI folding procedure was adopted from[2]. In essence, 1.5-2.5 mg of ligated material was dissolved in a minimal volume of 0.1M Tris, 6M Gdn-HCl, pH 8 and diluted with 1M Tris, 1M Gdn-HCl, pH 8.6 into to a final BPTI concentration of 0.2 mg/ml. The folding solution was stirred at RT in an open container under ambient O2 conditions. In the case of C14U BPTI, 0.6mg/ml of GSSG/GSH was added as to accelerate folding. Formation of folded protein was followed by analytical HPLC using a Vydac C18 column. After completion of folding, the BPTI variants were purified by HPLC using a 10mm x 250mm Vydac C18 column, analysed by LC-MS and lyophilised. Yield: 0.2-0.25 mg.

Recombinant expression of BSAP1.

The procedure for SECIS-free expression of selenoproteines was tailored from. E.coli strain β_UU3 was a kindly provided by Drs. Andrew Ellington and Ross Thyer (UT Austin, USA). pBAD33.1 plasmid was a gift from Christian Raetz (Addgene plasmid # 36267). Gene synthesis and cloning service was provided by GenScript. Genes of His6-SUMO-BSAP1 and its Sec containing mutants (Table S2) were cloned to pBAD33.1 by NdeI/HindIII sites and transfected to β_UU3 chemically competent cells.

A single colony of transfected β_UU3 cells was inoculated overnight at 37℃ in LB medium supplemented with 500 μg/ml ampicillin, 25 μg/ml chloramphenicol and 10 μM Na_2SeO_3. Overnight culture was diluted 1/200 by fresh LB medium and cultured further at 37℃ until OD600 reached 0.6-0.8. At that point, culture was cooled till 30℃ and induced by 0.2% L-arabinose. After overnight incubation, cells were harvested by centrifugation at 4000 rpm for 20 min at 4℃.

BSAP1 purification and folding.

For cell lysis, pellets were resuspended in lysis buffer (6M Gdn-HCl, 0.1M Tris, pH 8) at concentration 0.2g/ml and stirred for 1 hour at 4℃ followed by sonication. Insoluble debris were removed by centrifugation 10000 rpm for 20 min at 4℃. Cleared lysate was supplemented by

20mM imidazole, applied to Ni NTA Agarose (Quagen) and stirred for 1 hour at RT. Suspension was transferred to an empty PD10 column and filtered under mild vacuum. Ni NTA Agarose then was wash by 1 column volume of lysis buffer. Bound proteins were eluted by 1 column volume of 20mM phosphate, 500mM NaCl, 500mM imidazole, pH 7.4. Eluted fractions were dialysed against PBS, pH 7.4. In order to remove a His6-SUMO tag, 5U/ml of SUMO protease 1 (Sigma-Aldrich) and 0.6 mg of GSH were added and solution was gently stirred at 30°C until cleavage completed. After cleavage completion solution was adjusted by 6M Gdn-HCl, 0.1M Tris, pH 8 to final concentration of 1M Gdn-HCl, supplemented by 0.6mg/ml of GSSG and stirred at RT. The required BSAP1 variant was subsequently purified by HPLC using a 10mm x 250mm Vydac C18 column, analysed by LC-MS and lyophilised. Yield: ~0.1mg/L of LB culture.

NMR sample preparation

NMR samples of seleno-L-cystine and L-cystine (purchased from Sigma-Aldrich, MO) were prepared as saturated solution (weighed 40 mg powder in 1 ml 0.35N HCl) in 5 mm NMR tubes with added D_2O 5% (v/v) for deuterium lock.

NMR samples of Arg-Vasopressin wt, C1U, C6U and C1U/C6U were made in 5 mm NMR tubes as 1.6 mM solutions (0.55 ml volume) in 25 mM NaAc-d^3 buffer (pH 4.45), containing 0.1 mM EDTA, 0.2 mM sodium azide, 3 μM DSS-d^6 as chemical shift reference and 2% (v/v) D_2O for deuterium lock.

NMR samples of μ-conotoxin KIIIa, wt, C1U, C2U, and C4U were prepared in 3 mm tubes (160 μl volume) as 1.65 mM solutions in 25 mM NaAc-d^3 buffer (pH 4.45), containing 0.1 mM EDTA, 0.2 mM sodium azide, 3 μM DSS-d^6 as chemical shift reference and 2% (v/v) D_2O for deuterium lock.

NMR samples of Kalata B1, wt, C5U, C22U, C27U and C29U were made by dissolving freeze-dried peptide in 25 mM NaAc-d^3 buffer (pH 4.45), containing 0.1 mM EDTA and 0.2 mM sodium azide. Kalata B1 does not dissolve well above pH 3.5, but sufficiently enough upon lowering the solution pH to 3.0. The pH of the Kalata B1 NMR samples were adjusted to exactly pH 3.0, by adding small aliquots of 1N HCl resulting in a clear solution. pH values were measured using an Thermo Scientific Orion 3 Star pH-meter in combination with a Amani-1000L glassless micro-pH electrode from Innovative Design Inc (Tampa FL, USA). Final peptide concentration was 2.1 mM at 160 μl volume in a 3 mm tube, including a trace amount of DSS-d^6 as chemical shift reference and 2% (v/v) D_2O for deuterium lock. The C29U mutant has limited solubility at pH 3.0 when compared to the other Kalata B1 constructs and instead was dissolved up to a final concentration of approximately 1 mM.

BPTI variants were measured in standard 25 mM NaAc-d^3 buffer (pH 4.45) containing 0.1 mM EDTA, 0.2 mM sodium azide, 3 µM DSS-d^6 as chemical shift reference and 2% (v/v) D_2O for deuterium lock. The final concentrations of the four BPTI samples in 3 mm tubes (160 µl volume) was dependent on available amount of purified protein, and were 0.35 mM for wt, 0.18 mM for C5U, and 0.2 mM for both C14U and C30U. However, BPTI is a rigid monomeric protein structure and chemical shifts checked out to be concentration-independent.

NMR samples of truncated Evasin3 (tEv3 17-56) were prepared in the same buffer as µ-conotoxin KIIIa. Final sample concentrations were: 0.7 mM for tEv3 wt and tEv3-SecAll, and 1.2-1.4 mM for tEv3 C22U, C26U and C33U. All tEv3 samples were prepared in 3 mm NMR tubes (160 µl volume).

NMR samples of BSAP-1 wt, C18U and C22U were made by dissolving freeze-dried, folded protein into 160 µl KPi D2O buffer 25 mM (pH 7.1) including 0.1 mM EDTA, 0.2 mM sodium azide and trace amount of DSS-d^6, and measured in 3 mm NMR tubes. Final protein concentrations were 228, 156 and 192 µM for wt, C18U and C22U, respectively.

NMR spectroscopy

NMR spectra were acquired on a Bruker Avance III HD 700 MHz spectrometer, equipped with a TCI [^{13}C,^{15}N,^{1}H] cryoprobe. Probe temperature was set to 37 °C, except for Arg-vasopressin and BPTI where spectra were recorded at 25°C, whereas BSAP-1 samples were recorded at 30 °C to achieve optimal spectral resolution. There were two reasons to lower the temperature; the first one is reduced overlap of Hα resonances with the residual water line in HSQC 13C-1H spectra. The other reason is that BPTI shows less relaxation losses at 25 °C because of dynamic exchange broadening of important C14 and C38 resonances at elevated temperatures[3].

Typically for every peptide and protein a complete series of 2D spectra were recorded to assign most ^{1}H, ^{13}C (non-carbonyl) and ^{15}N resonances. The standard series is made off a ^{1}D ^{1}H spectrum, and various 2D spectra: DIPSI, NOESY, natural abundance ^{13}C-^{1}H HSQC (optimized for both the aromatic and aliphatic region), ^{13}C-^{1}H HSQC-DIPSI and ^{15}N-^{1}H HSQC. Initially, the DIPSI and NOESY spectrum were used for sequential assignment of backbone and other side chain protons, after which the assigned protons were connected up to their respective ^{15}N and ^{13}C nuclei via the corresponding heteronuclear HSQC correlation spectra. Stereospecific assignments of prochiral methyl and methylene groups were not analyzed per se and chemical shifts of prochiral proton pairs are reported ordered on basis of their relative chemical shift position. In case of the smaller and more concentrated peptides, Arg-vasopressin and µ-conotoxin KIIIa, ^{13}C-^{1}H HMBC spectra provided additional assignments for carbonyl ^{13}CO chemical shifts.

The mixing time for the DIPSI experiments was set to 80 ms, the mixing time of the NOESY spectra was chosen properly according apparent to molecular weight, and was set to 400 ms for vasopressin and μ-conotoxin KIIIa, 300 ms for Kalata B1, 200 ms for tEv3 and 150 ms for BPTI. Water suppression in the ^{1}D ^{1}H and 2D homonuclear spectra was carried out using excitation sculpting[4], while gradient sensitivity-enhanced versions of ^{13}C-^{1}H HSQC, ^{13}C-^{1}H HSQC-DIPSI with 35 or 70 ms mixing time, and ^{15}N-^{1}H HSQC (flip back version), taken from the Bruker pulse sequence library, were used throughout. For the ^{13}C-^{1}H HMBC spectra in water, a gradient, non-decoupled, triple band-pass filter pulse sequence was used, with additional presaturation of the water line during the relaxation time. Optimization for the detection of long-range couplings between proton and carbon resonances in the HMBC was set to 10 Hz.

Typically, the total measurement time to run a series spectra on one of the vasopressin samples at 2 mM concentration typically took approximately 24 hours, with most of the time spent on the natural abundance heteronuclear ^{15}N and ^{13}C ^{2}D HSQC spectra. On the other hand, a well-resolved aliphatic version of the ^{13}C-^{1}H HSQC spectrum to detect the important Sec/Cys Hβ-Cβ correlations on samples like BPTI C14U (containing some 0.2 mg protein material) consumed about 40 hrs experiment time on our 700 MHz spectrometer.

Chemical shift assignments of BSAP-1 wt resonances were initially made using standard triple resonance experiments and HCCH-DIPSI spectra on expressed [^{13}C,^{15}N] BSAP-1 in similar water buffer as listed for the BSAP-1 Sec mutants. Because of the broad resonance lines in combination with the relatively low concentration of the protein in solution, a 2D DIPSI (mixing time 70 ms) and a natural abundance ^{13}C-^{1}H HSQC spectrum of reference BSAP wt, C18U and C22U were recorded in pure D_2O (99.9%) buffer to avoid strong interference of the water line in detecting Hα–Cα proton correlations. Chemical shift positions of mutant BSAP-1 turn out very similar to that of wt, and proton and carbon shifts of the mutants could be assigned through chemical shift analogy. Plotted chemical shift differences of carbons in BSAP-1 C18U and C22U are based on comparison with reference BSAP-1 (228 μM) in D_2O.

Additional proton-decoupled ^{77}Se spectra on selenocystine and Arg-vasopressin Sec samples were recorded on a Bruker Avance III 500 MHz spectrometer, equipped with a cryogenically cooled BBO probe, capable of tuning on a ^{77}Se frequency of 95.40 MHz. ^{1}H-^{77}Se correlated spectra were recorded using a gradient-based long-range HSQC pulse sequence and/or using Pure-In-Phase (PIP) HSQMBC spectra[5]. These latter two pulse sequences are normally dedicated to detect carbon correlations, but have been modified here by adapting the gradient ratios towards ^{77}Se instead of ^{13}C. Optimal transfer delays corresponding to the two-band coupling constants between Hβ1 and Hβ2 proton and ^{77}Se were derived from the passive ^{77}Se splittings that are present as E.COSY

patterns inside ^{13}Cβ-Hβ1/Hβ2 HSQC correlation peaks e.g. in the acidified saturated selenocystine NMR sample. Values of 2J -12.7 Hz and -19.0 Hz for resp. Hβ1 and Hβ2 to ^{77}Se were measured in selenocystine. PIP-HSQMBC spectra on the same selenocystine sample indicate somewhat larger values for ^{2}J(Hβ2-^{77}Se) of -22 Hz, and in addition indicates a ^{3}J(Hα-^{77}Se) of ca. 7-8 Hz. Detection sensitivity for long-range detection of Sec/Cys Hα and Hβ resonances to ^{77}Se nuclei appears rather low, even on a cryoprobe. Already at a maximum usable transfer delay equivalent to a coupling of 32 Hz, severe magnetization losses occur as a result of efficient relaxation of the broad ^{77}Se resonance lines. Besides selenocystine (>10 mM) only the smaller-sized vasopressin peptide samples gave useful ^{77}Se 1D and 2D spectra. However, Hβ to ^{77}Se correlations were exclusively observed over the two bonds, intra-Sec coupling step, rather than over the inter-Sec coupling that reaches across the bridged Se-Se or S-Se bond (estimated upper limit of ^{3}J(^{1}H-^{77}Se) based on ^{77}Se satellite 1D proton spectra < 2 Hz). ^{77}Se chemical shifts are referenced externally to diphenyl-diselenide in $CDCl_3$.

Spectral processing was done by Topspin 3.2 (Bruker GmbH, Rheinstetten, Germany) spectral analysis and resonance assignment was carried out by Sparky 3.1156. Zero-filling and forward linear prediction was routinely used before each Fourier transformation to increased spectral resolution in the indirect dimensions of the 2D spectra.

Mass spectrometry.

UPLC ESI-MS was performed on a Waters UHPLC XEVO-G2QTOF system. Peptide masses were calculated from the experimental mass to charge (m/z) ratios of all the protonation states observed in the ESI-MS spectrum of a peptide. Monoisotopic and average theoretical masses of compounds were calculated using Peptide Mass Calculator (Peptide Protein Research Ltd) in combination with Chemdraw 12.0.2.

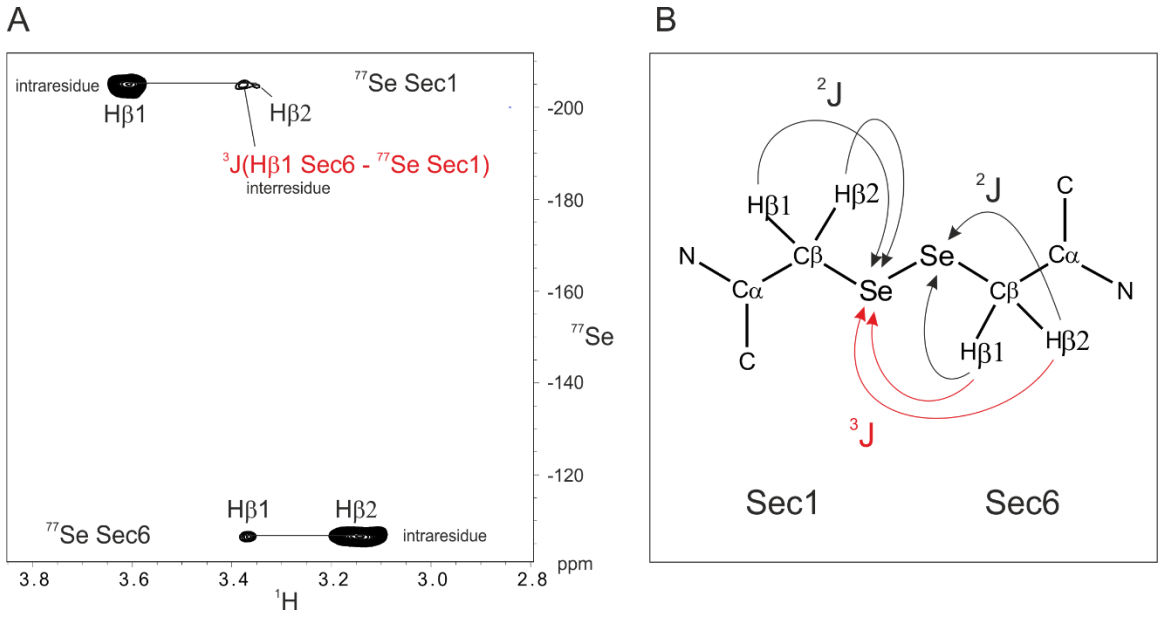

Fig. S1. NMR analysis of Arg-vasopressin Sec1/Sec6

A. ^{1}H-^{77}Se HSQC spectrum of Arg-vasopressin Sec1/Sec6, recorded on a 500 MHz 1H spectrometer, and optimized for the detection of long-range scalar ^{1}H-^{77}Se coupling constants. Intra residual ^{2}J coupling constants between beta protons Hβ1 and Hβ2 Sec1 and ^{77}Se Sec1 and between Hβ1 and Hβ2 Sec6 and ^{77}Se Sec6 are easily observed in the spectrum. A weak cross corresponding to the inter residual ^{3}J coupling constants between ^{77}Se Sec1 and the Hβ1 protons of Sec6 across the Se-Se bond is visible in the spectrum, and partially overlaps with the stronger ^{2}J correlated peaks. B. Schematic representation of coupling pathways.

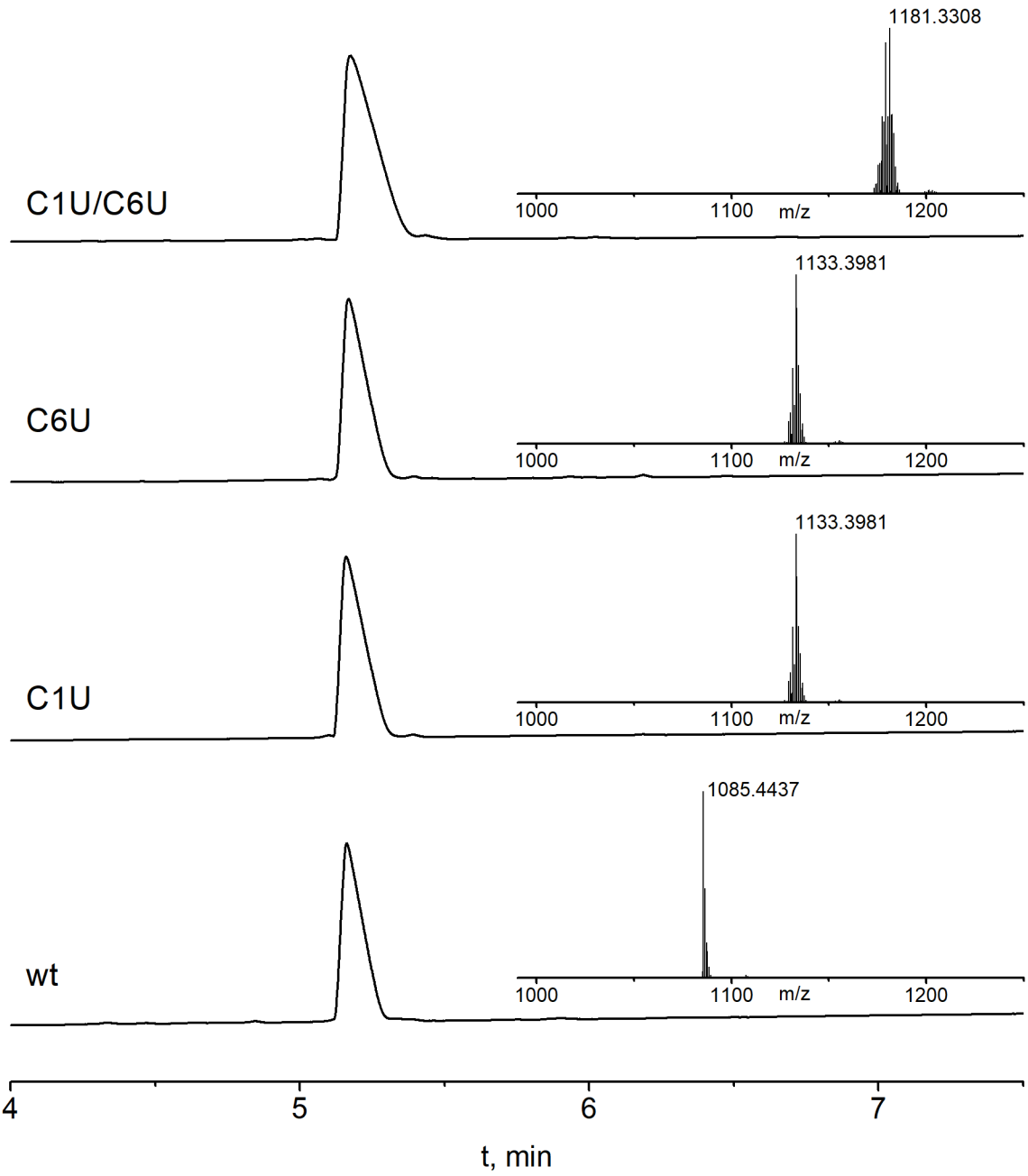

Fig. S2. LC-MS analysis of purified Arg-vasopressin variants.

Profiles of Arg-Vasopressin C1U/C6U, C6U and C1U, in comparison to that of wild-type (wt) Arg-vasopressin.

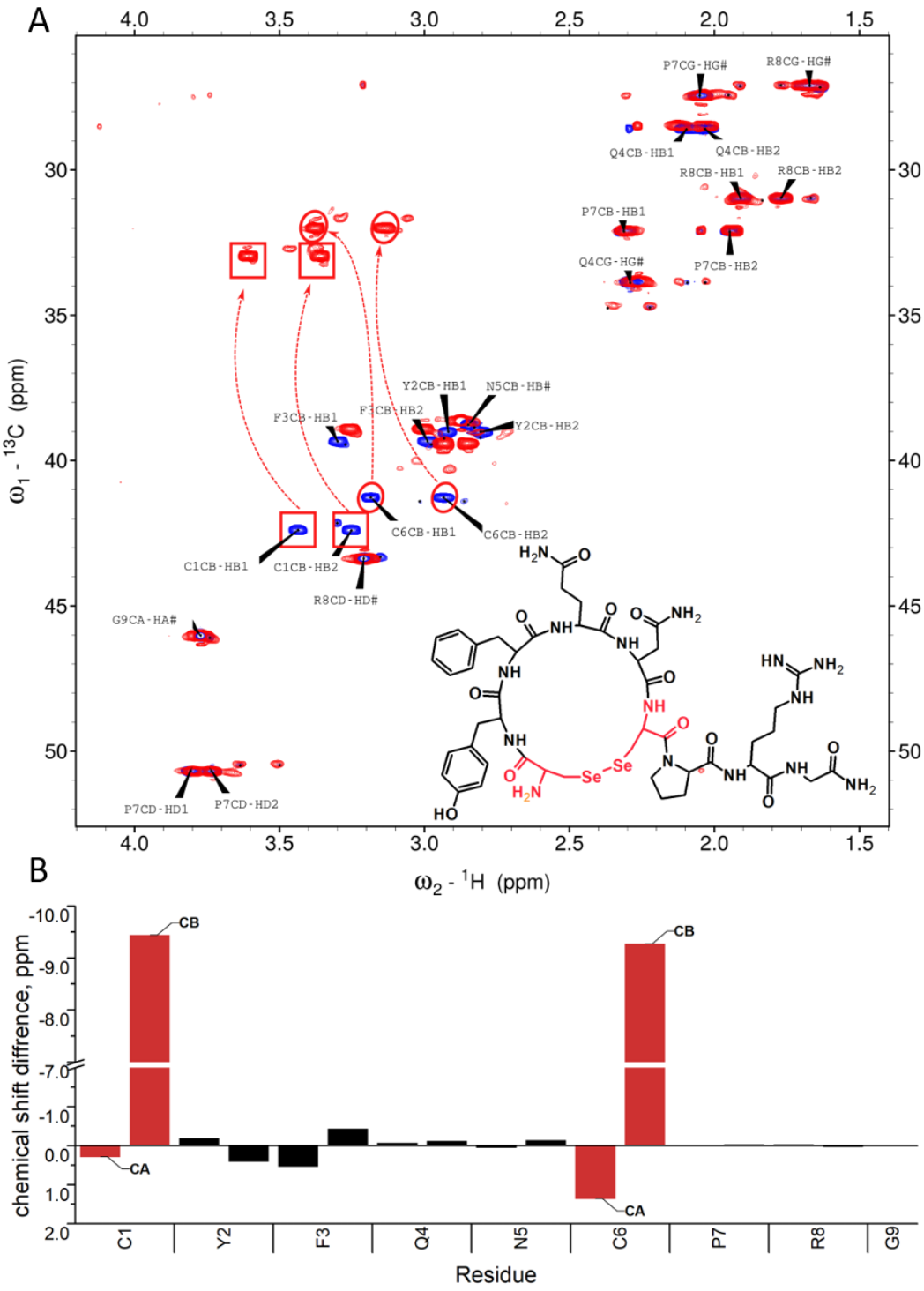

Fig. S3. Chemical shift perturbations induced by Se in C1U/C6U Arg-vasopressin.
A. Overlaid ^{1}H-^{13}C HSQC spectra of wt (blue) and C1U/C6U Arg-vasopressin (red). Squares show the displacements of Hβ1/2-Cβ peaks of U1, ellipses display Hβ1/2-Cβ peaks of the opposite U6 residue. B. Chemical shift difference plot of assigned carbon atoms in wt and C1U/C6U Arg-vasopressin. Delta values derived for U1 and U6 are coloured red.

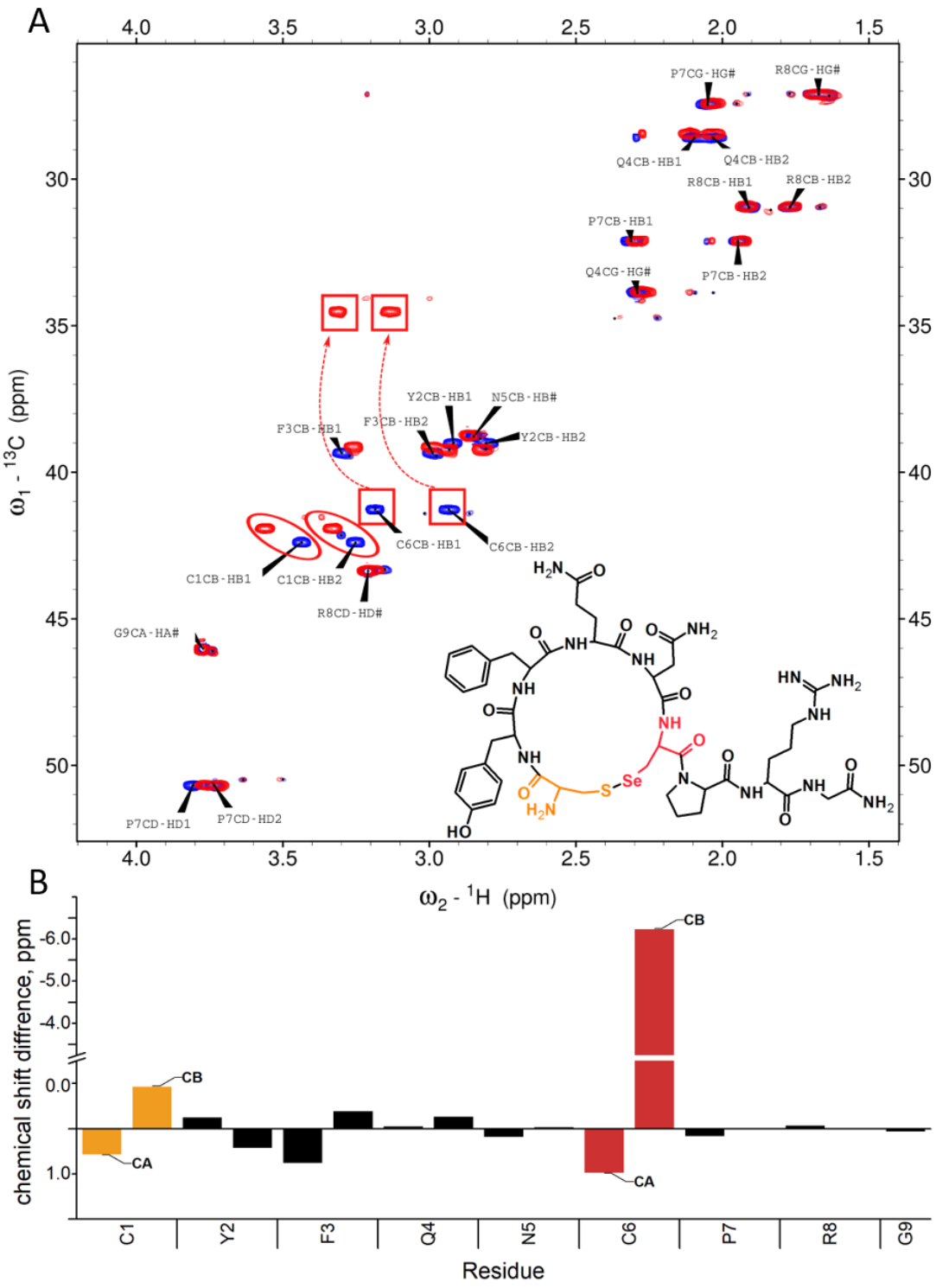

Fig. S4. Chemical shift perturbations induced by Se in C6U Arg-vasopressin.

A. Overlaid ^{1}H-^{13}C HSQC spectra of wt (blue) and C6U Arg-vasopressin (red). Squares show the displacements of Hβ1/2-Cβ peaks of U6, ellipses display Hβ1/2-Cβ peaks of the opposite C1 residue. **B.** Chemical shift difference plot of assigned carbon atoms in wt and C6U Arg-vasopressin. Delta values derived for U6 are coloured red, C1 values are coloured yellow.

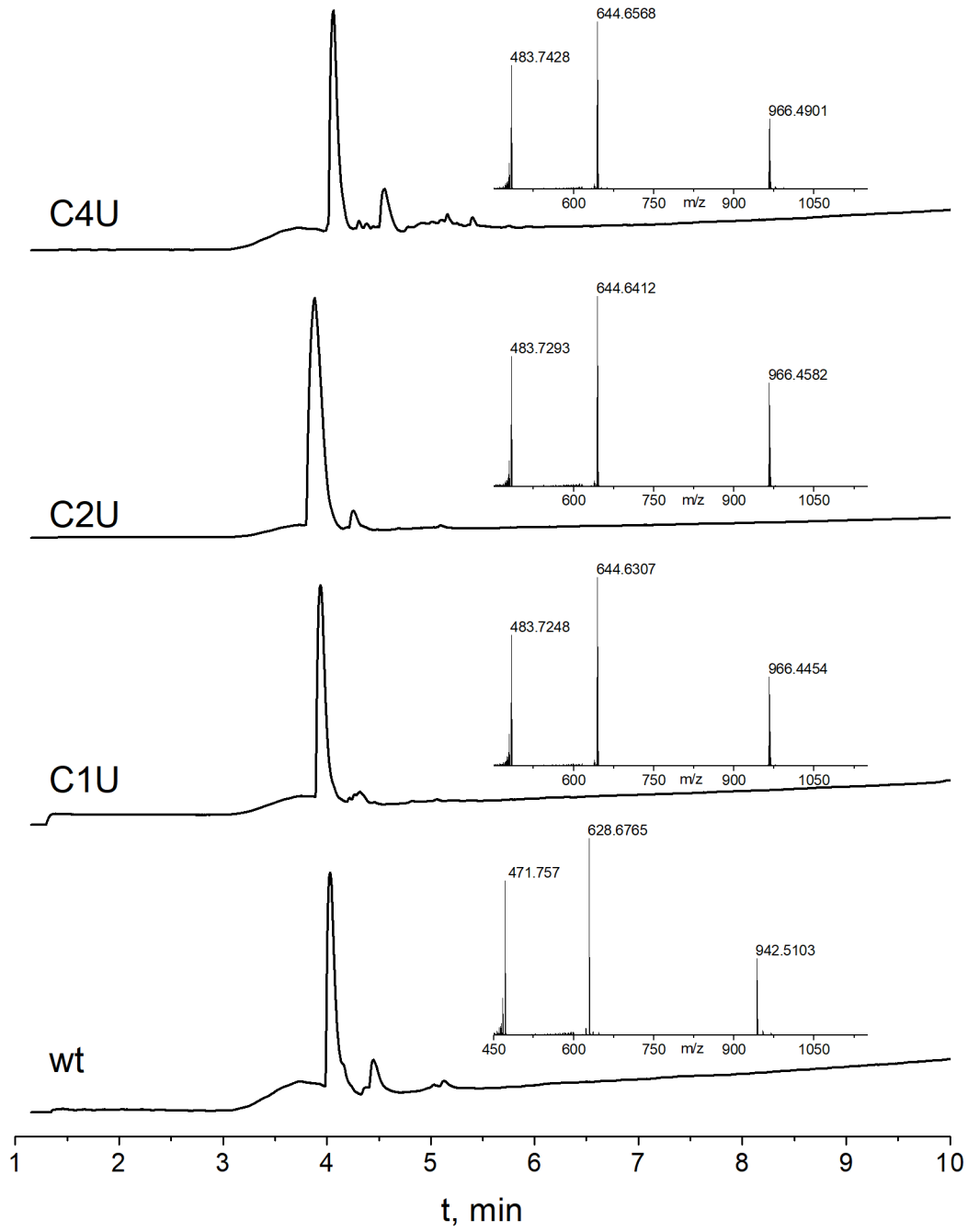

Fig. S5. LC-MS analysis of purified µ-conotoxin KIIIA variants.

Profiles of µ-conotoxin KIIIA C4U, C2U, and C1U, in comparison to that of wild-type (wt) µ-conotoxin KIIIA.

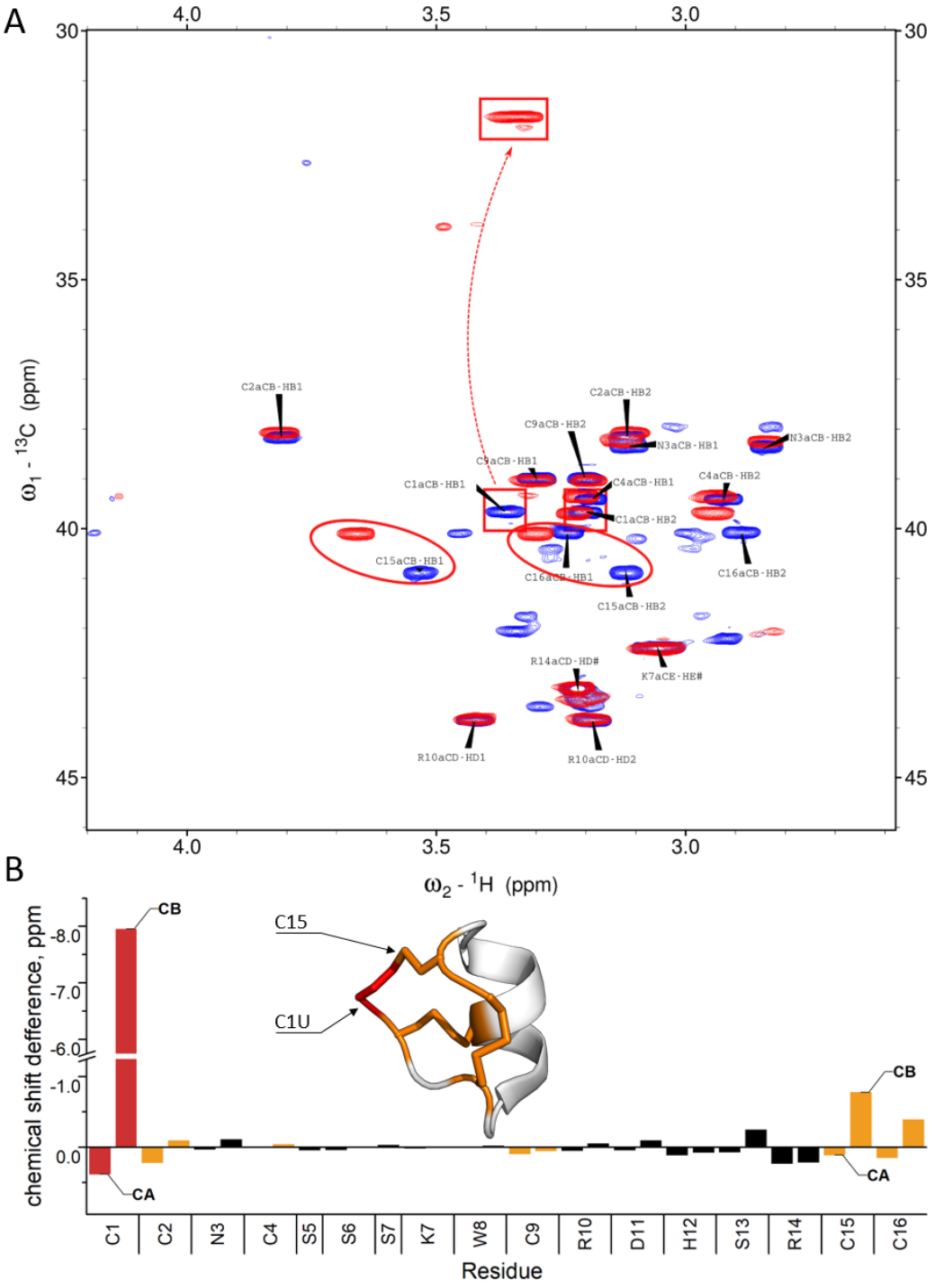

Fig. S6. Chemical shift perturbations induced by Se in C1U μ-conotoxin KIIIA.

A. Overlaid ^{1}H-^{13}C HSQC spectra of wt (blue) and C1U μ-conotoxin KIIIA (red). Squares show the displacements of Hβ1/2-Cβ peaks of U1, ellipses display Hβ1/2-Cβ peaks of the opposite C15 residue. Unlabelled peaks represent the presence of minor form of μ-conotoxin KIIIA with non-natural disulphide connectivity due to poor separation, as was reported earlier[7]. B. Chemical shift difference plot of assigned carbon atoms in wt and C1U μ-conotoxin KIIIA. Delta values derived for U1 are coloured red, values for other cysteines are coloured yellow.

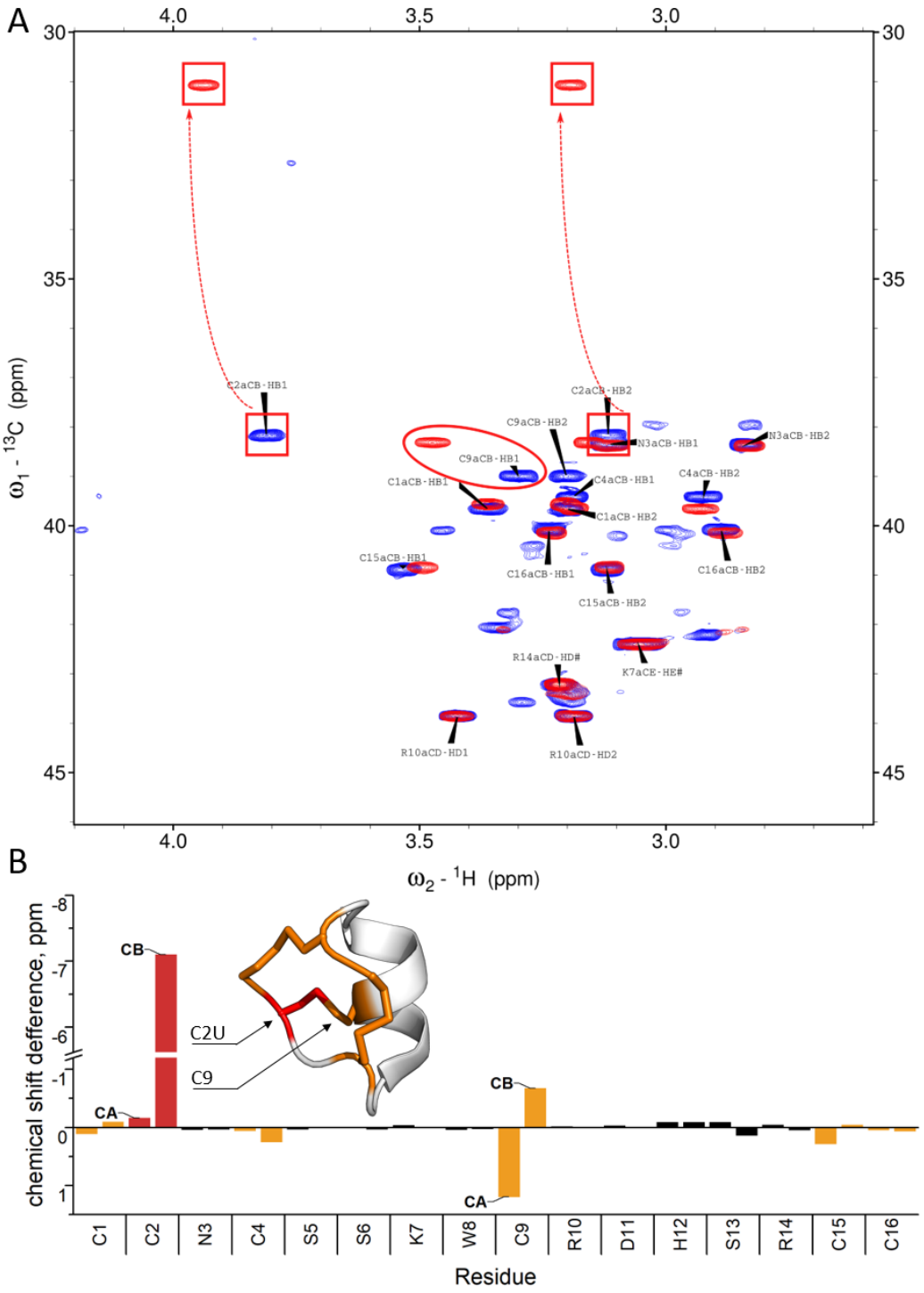

Fig. S7. Chemical shift perturbations induced by Se in C2U μ-conotoxin KIIIA.

A. Overlaid ^{1}H-^{13}C HSQC spectra of wt (blue) and C2U μ-conotoxin KIIIA (red). Squares show the displacements of Hβ1/2-Cβ peaks of U2, ellipses display Hβ1-Cβ peak of the opposite C9 residue. Unlabelled peaks represent the presence of minor form of μ-conotoxin KIIIA with non-natural disulphide connectivity due to poor separation, as was reported earlier[7]. B. Chemical shift difference plot of assigned carbon atoms in wt and C1U μ-conotoxin KIIIA. Delta values derived for U2 are coloured red, values for other cysteines are coloured yellow.

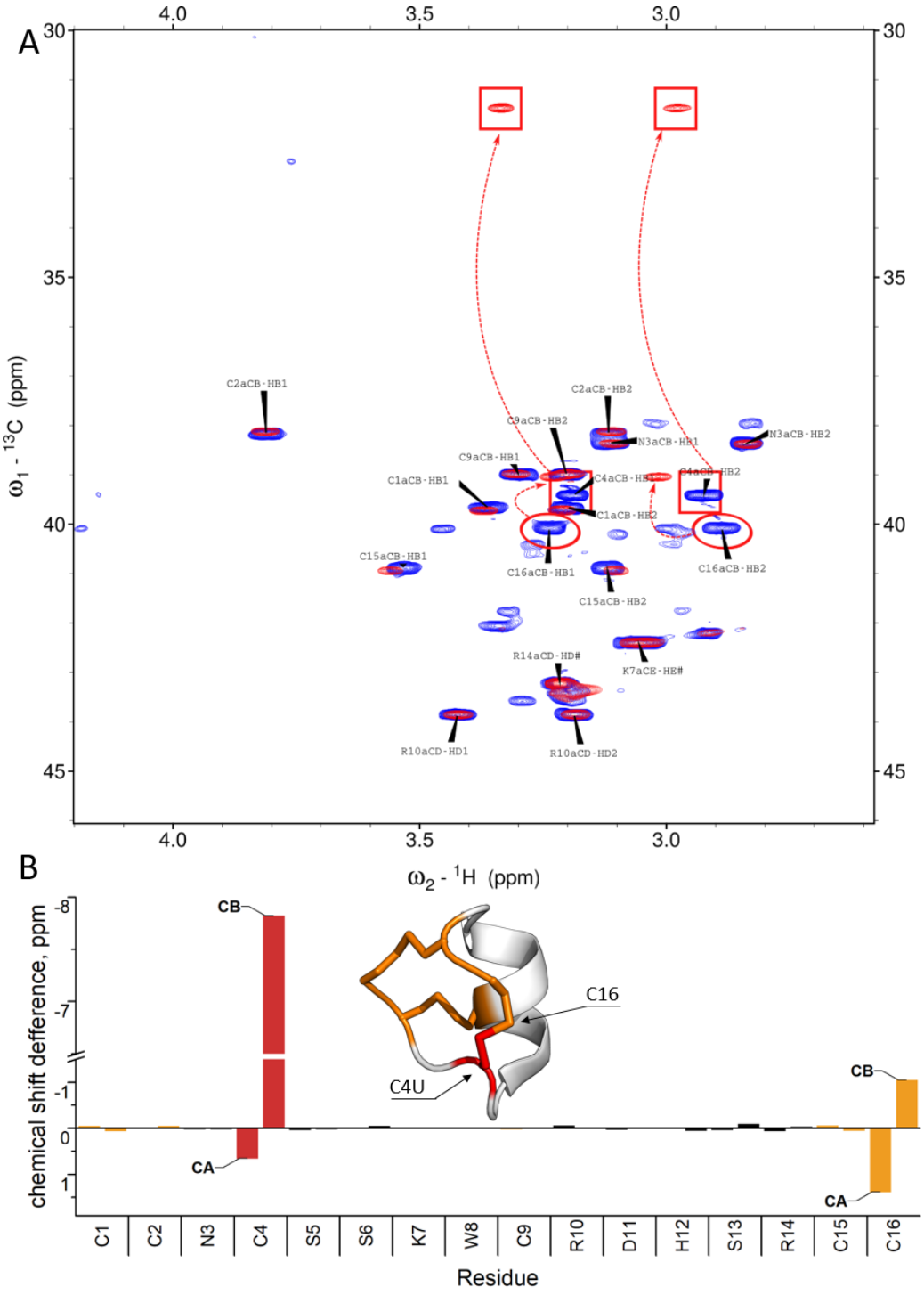

Fig. S8. Chemical shift perturbations induced by Se in C4U μ-conotoxin KIIIA.

A. Overlaid ^{1}H-^{13}C HSQC spectra of wt (blue) and C2U μ-conotoxin KIIIA (red). Squares show the displacements of Hβ1/2-Cβ peaks of U4, ellipses display Hβ1-Cβ peak of the opposite C16 residue. Unlabelled peaks represent the presence of minor form of μ-conotoxin KIIIA with non-natural disulphide connectivity due to poor separation, as was reported earlier[7]. B. Chemical shift difference plot of assigned carbon atoms in wt and C4U μ-conotoxin KIIIA. Delta values derived for U4 are coloured red, values for other cysteines are coloured yellow.

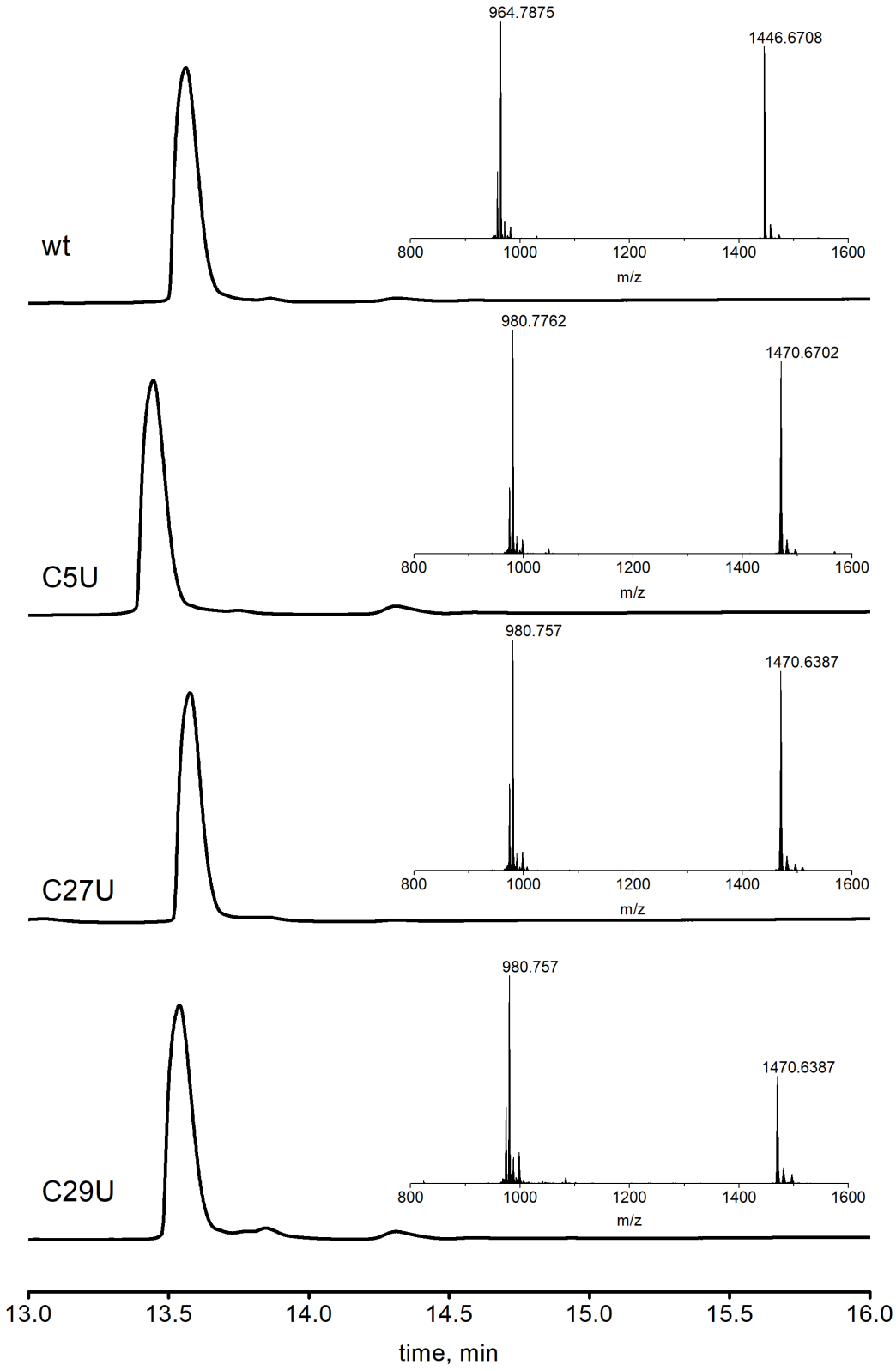

Fig. S9. LC-MS analysis of purified Kalata B1 variants.
Profiles of Kalata B1 C5U, C27U, and C29U, in comparison to that of wild-type (wt) Kalata B1.

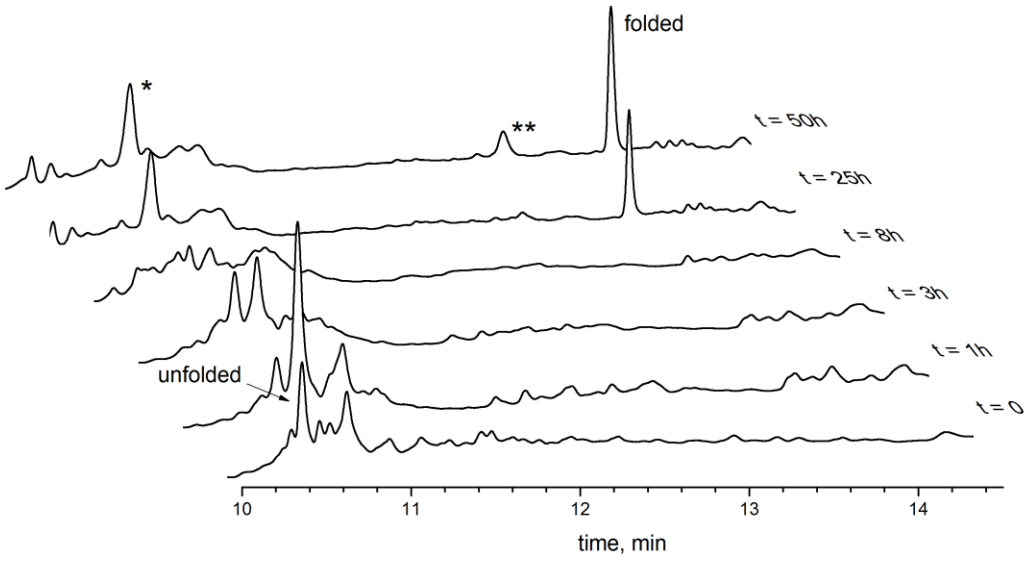

Fig. S10. Folding kinetics of wt Kalata B1.

HPLC chromatograms of folding progression of wt Kalata B1 recorded at different time points. * indicates misfolded Kalata B1; ** indicates a +56 adduct.

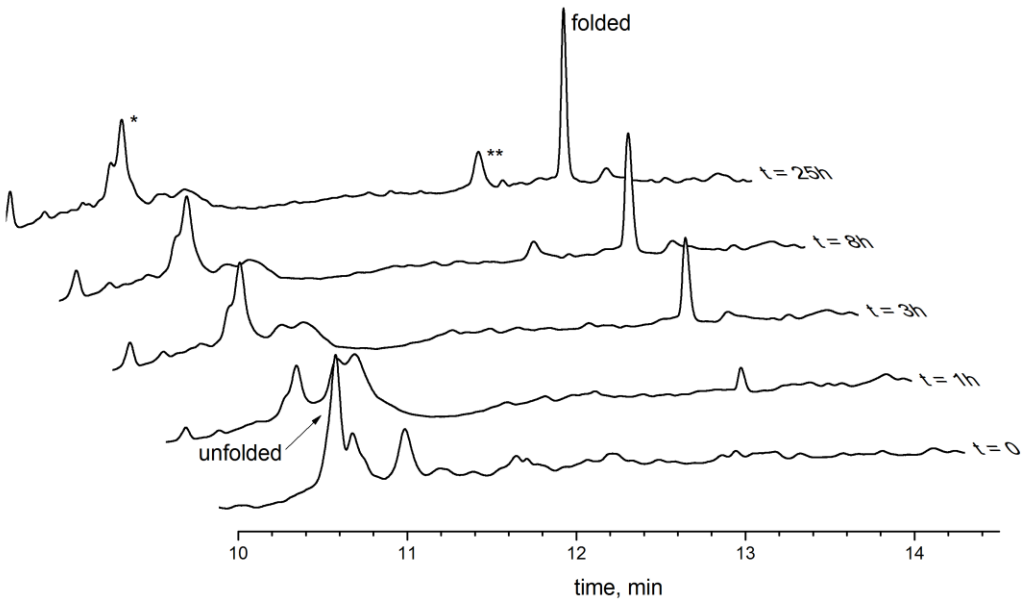

Figure S11. Folding kinetics of C5U Kalata B1.

HPLC chromatograms of folding progression of C5U Kalata B1 recorded at different time points. * indicates misfolded Kalata B1; ** indicates a +56 adduct.

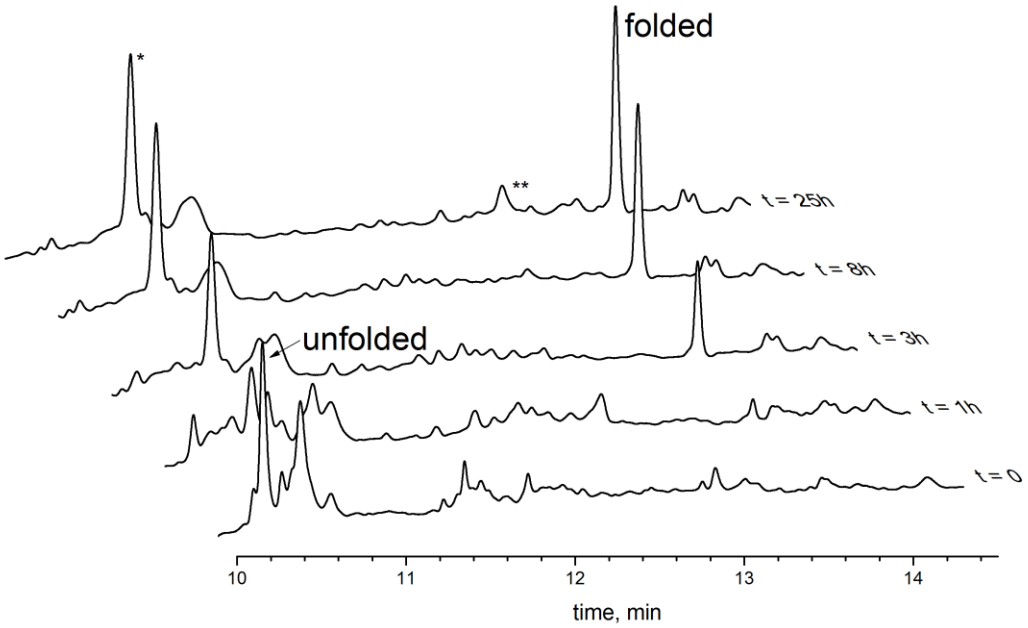

Figure S12. Folding kinetics of C22U Kalata B1.

HPLC chromatograms of folding progression of C22U Kalata B1 recorded at different time points. * indicates misfolded Kalata B1; ** indicates a +56 adduct.

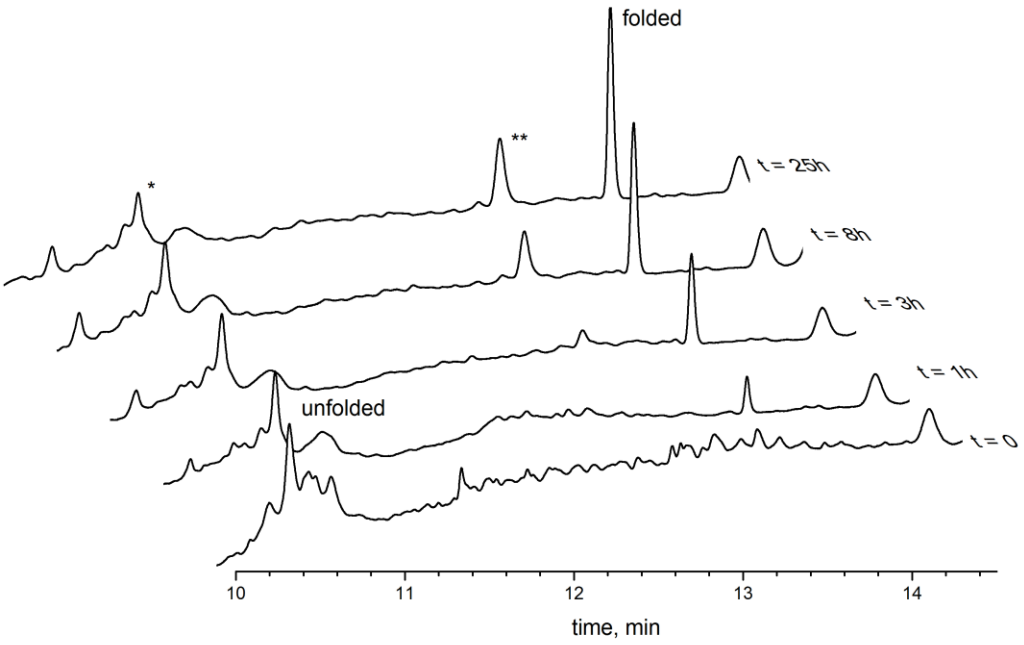

Figure S13. Folding kinetics of C27U Kalata B1.

HPLC chromatograms of folding progression of C27U Kalata B1 recorded at different time points. * indicates misfolded Kalata B1; ** indicates a +56 adduct.

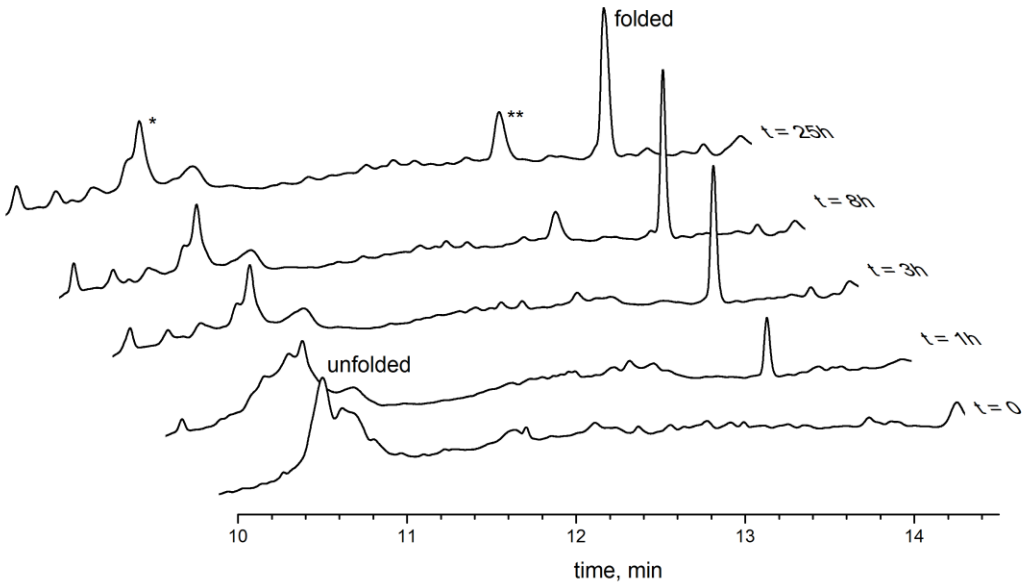

Figure S14. Folding kinetics of C29U Kalata B1.

HPLC chromatograms of folding progression of C29U Kalata B1 recorded at different time points. * indicates misfolded Kalata B1; ** indicates a +56 adduct.

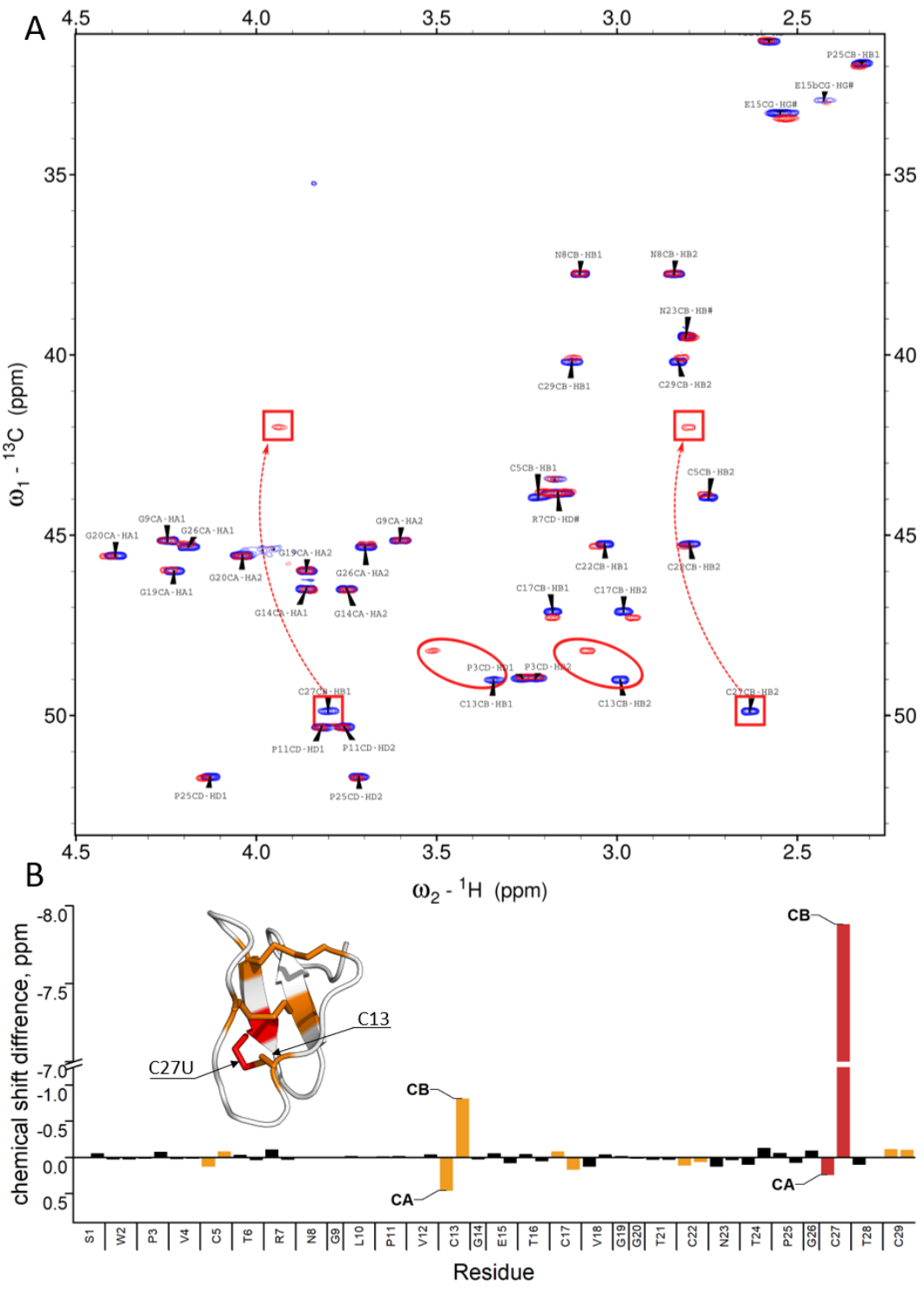

Figure S15. Chemical shift perturbations induced by Se in C27U Kalata B1.

A. Overlaid ^{1}H-^{13}C HSQC spectra of wt (blue) and C27U Kalata B1 (red). Squares show the displacements of Hβ1/2-Cβ peaks of U27, ellipses display Hβ1/2-Cβ peak of the opposite C13 residue. B. Chemical shift difference plot of assigned carbon atoms in wt and C27U Kalata B1. Delta values derived for U27 are coloured red, values for other cysteines are coloured yellow.

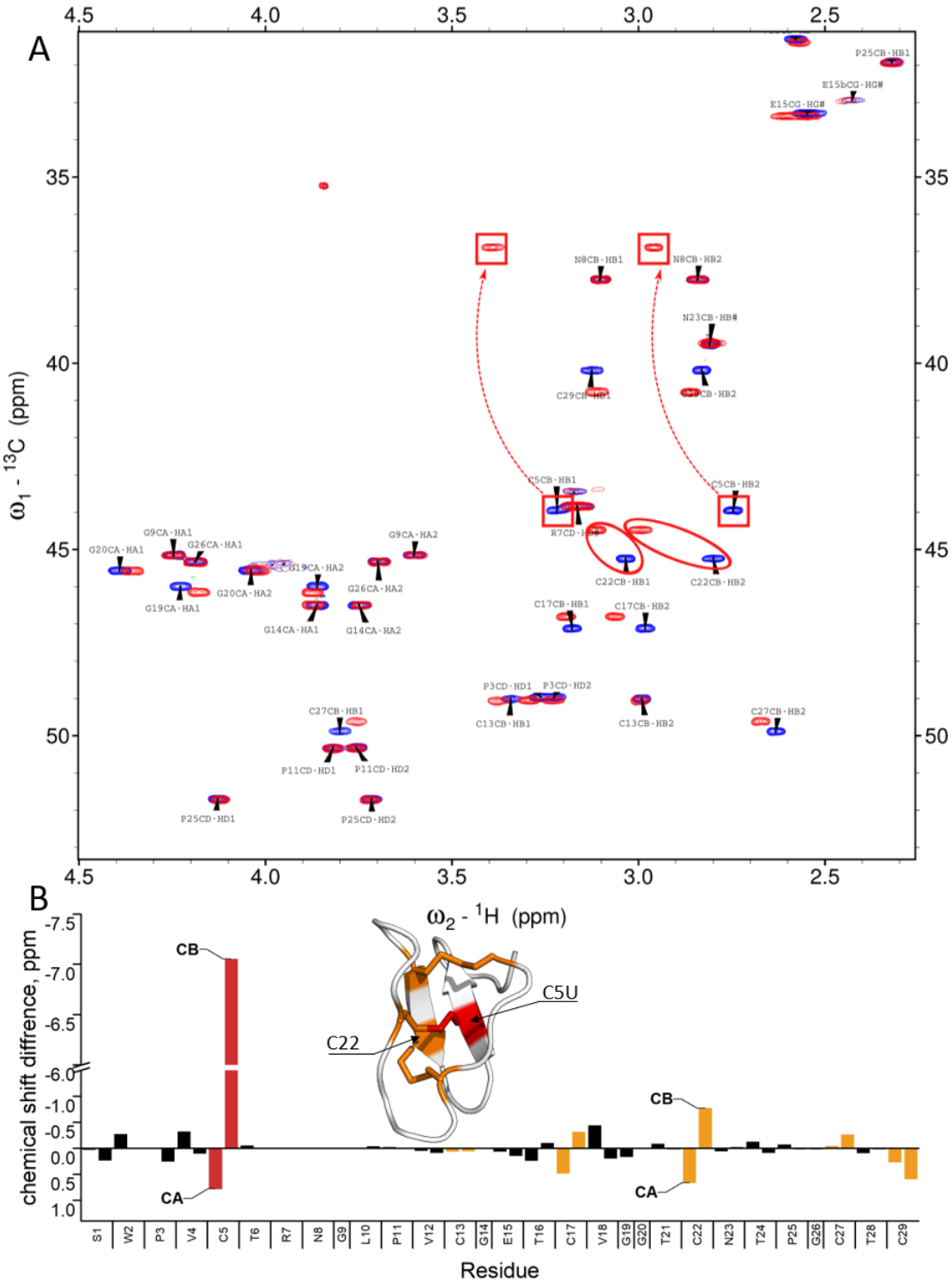

Figure S16. Chemical shift perturbations induced by Se in C5U Kalata B1.

A. Overlaid ^{1}H-^{13}C HSQC spectra of wt (blue) and C5U Kalata B1 (red). Squares show the displacements of Hβ1/2-Cβ peaks of U5, ellipses display Hβ1/2-Cβ peak of the opposite C22 residue. B. Chemical shift difference plot of assigned carbon atoms in wt and C27U Kalata B1. Delta values derived for U5 are coloured red, values for other cysteines are coloured yellow

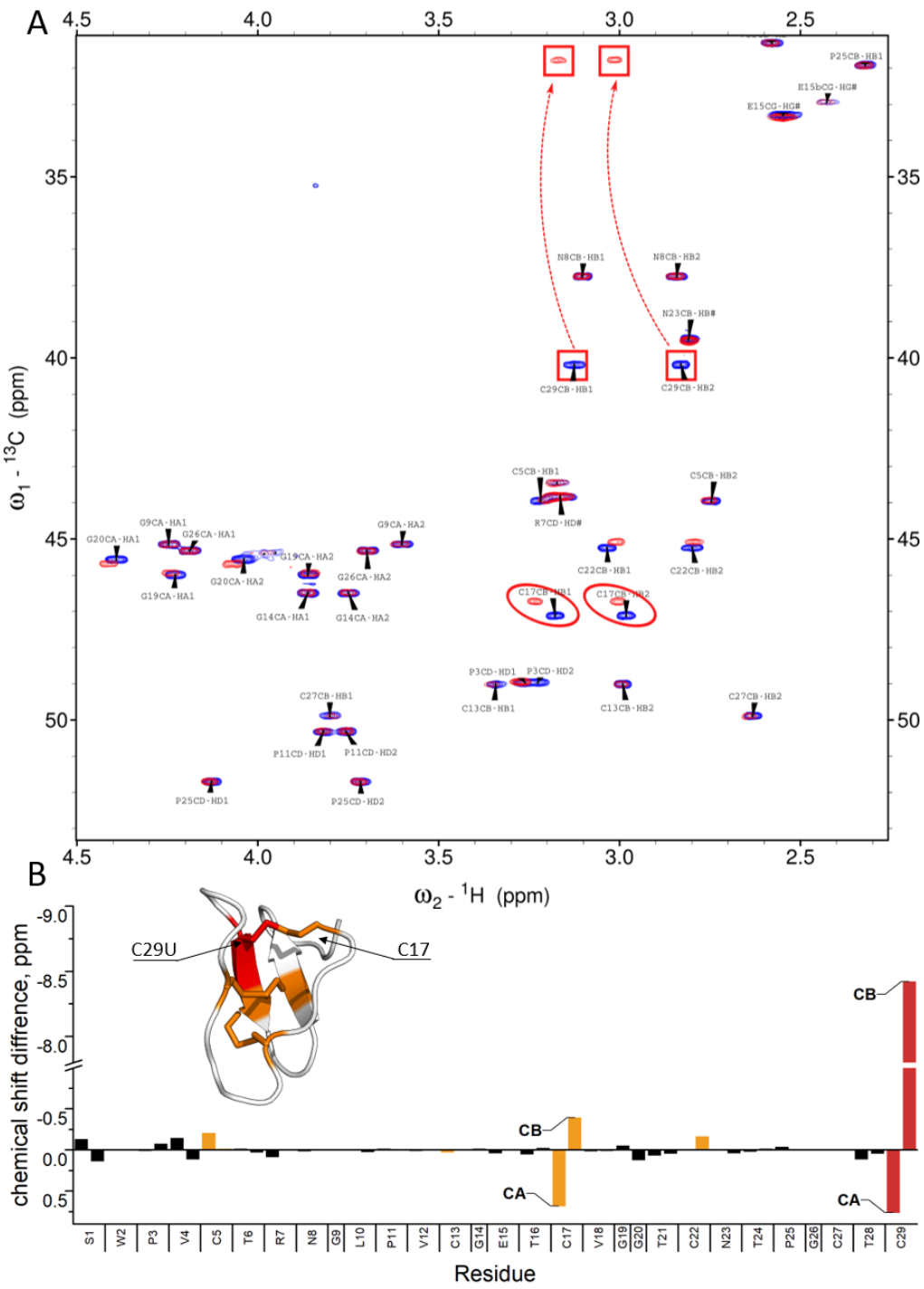

Figure S17. Chemical shift perturbations induced by Se in C29U Kalata B1.

A. Overlaid ^{1}H-^{13}C HSQC spectra of wt (blue) and C27U Kalata B1 (red). Squares show the displacements of Hβ1/2-Cβ peaks of U29, ellipses display Hβ1/2-Cβ peak of the opposite C17 residue. B. Chemical shift difference plot of assigned carbon atoms in wt and C29U Kalata B1. Delta values derived for U29 are coloured red, values for other cysteines are coloured yellow.

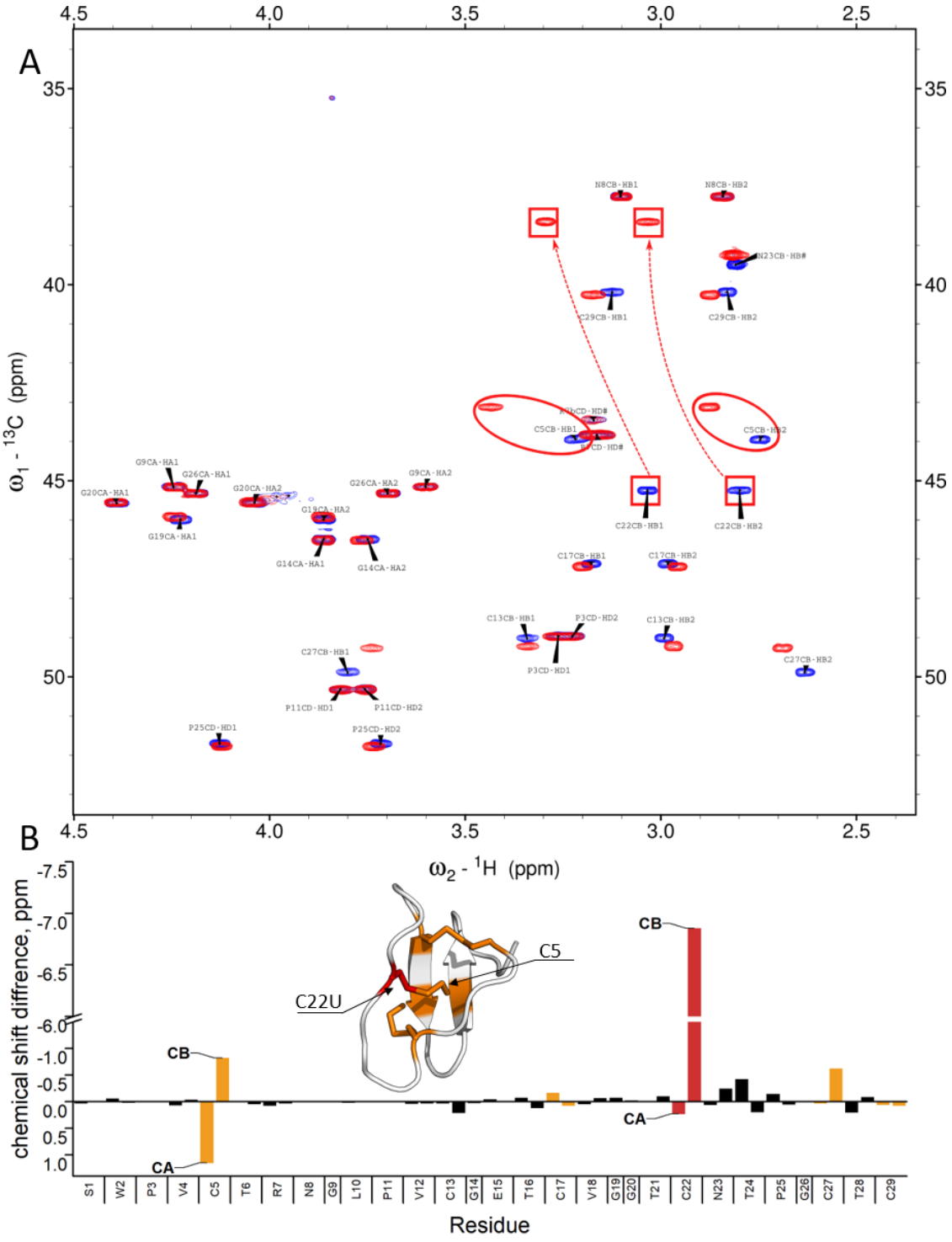

Figure S18. Chemical shift perturbations induced by Se in C22U Kalata B1.

A. Overlaid ^{1}H-^{13}C HSQC spectra of wt (blue) and C22U Kalata B1 (red). Squares show the displacements of Hβ1/2-Cβ peaks of U22, ellipses display Hβ1/2-Cβ peak of the opposite C5 residue. B. Chemical shift difference plot of assigned carbon atoms in wt and C27U Kalata B1. Delta values derived for U22 are coloured red, values for other cysteines are coloured yellow.

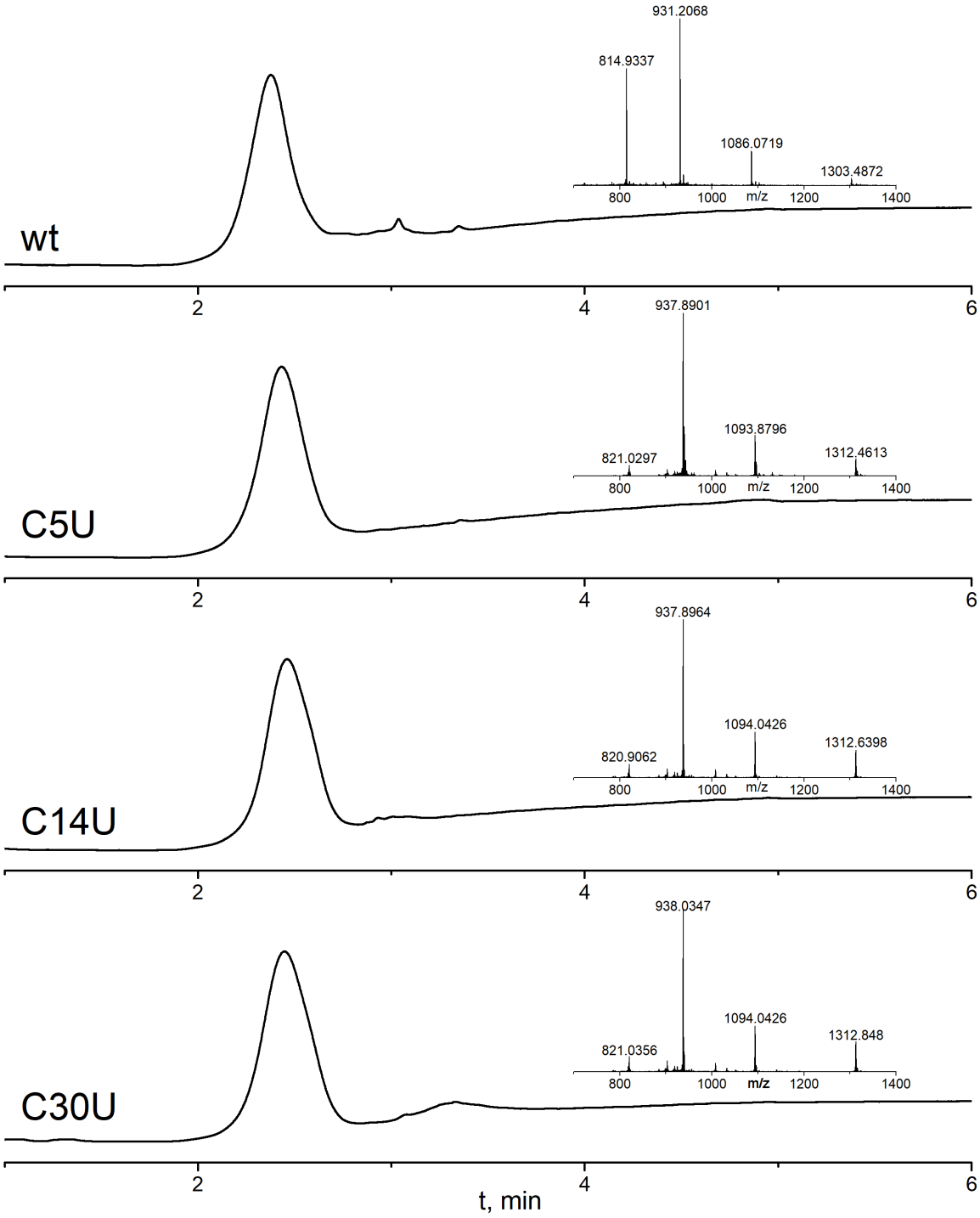

Figure S19. LC-MS analysis of purified BPTI variants.
Profiles of BPTI C5U, C14U, and C30U, in comparison to that of wild-type (wt) BPTI.

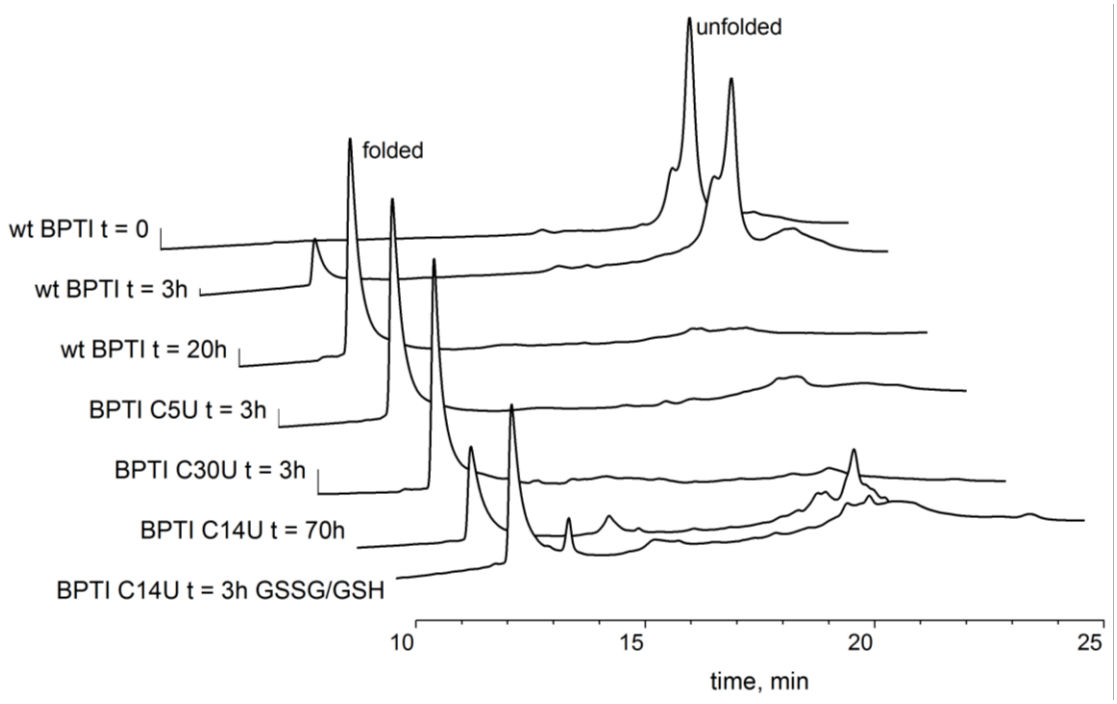

Figure S19. HPLC chromatograms of BPTI variants folding progression recorded at different time points during folding.

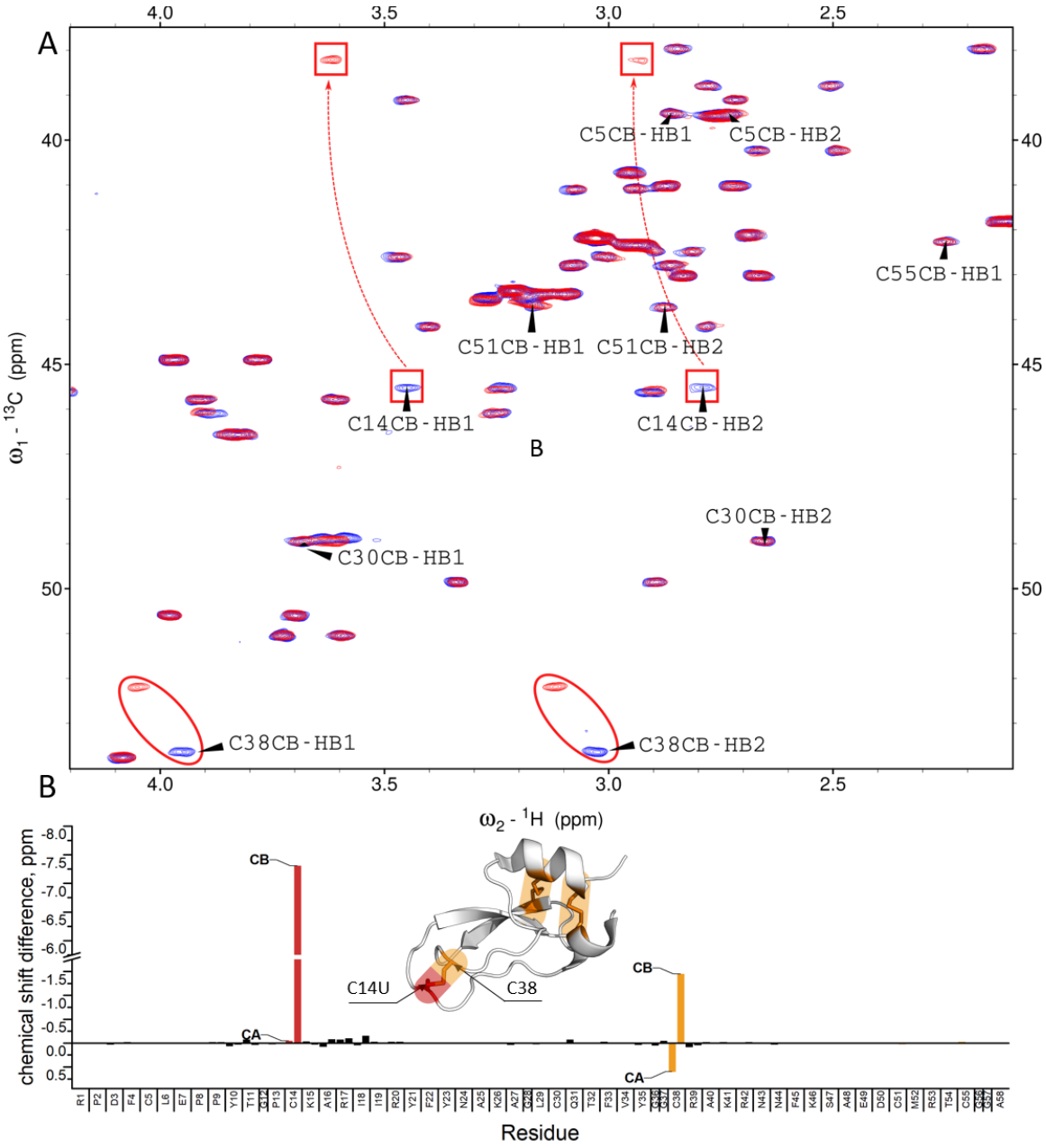

Figure S20. Chemical shift perturbations induced by Se in C14U BPTI.

A. Overlaid ^{1}H-^{13}C HSQC spectra of wt (blue) and C14U BPTI (red). Squares show the displacements of Hβ1/2-Cβ peaks of U14, ellipses display Hβ1/2-Cβ peak of the opposite C38 residue. B. Chemical shift difference plot of assigned carbon atoms in wt and C14U BPTI. Delta values derived for U14 are coloured red, values for other cysteines are coloured yellow.

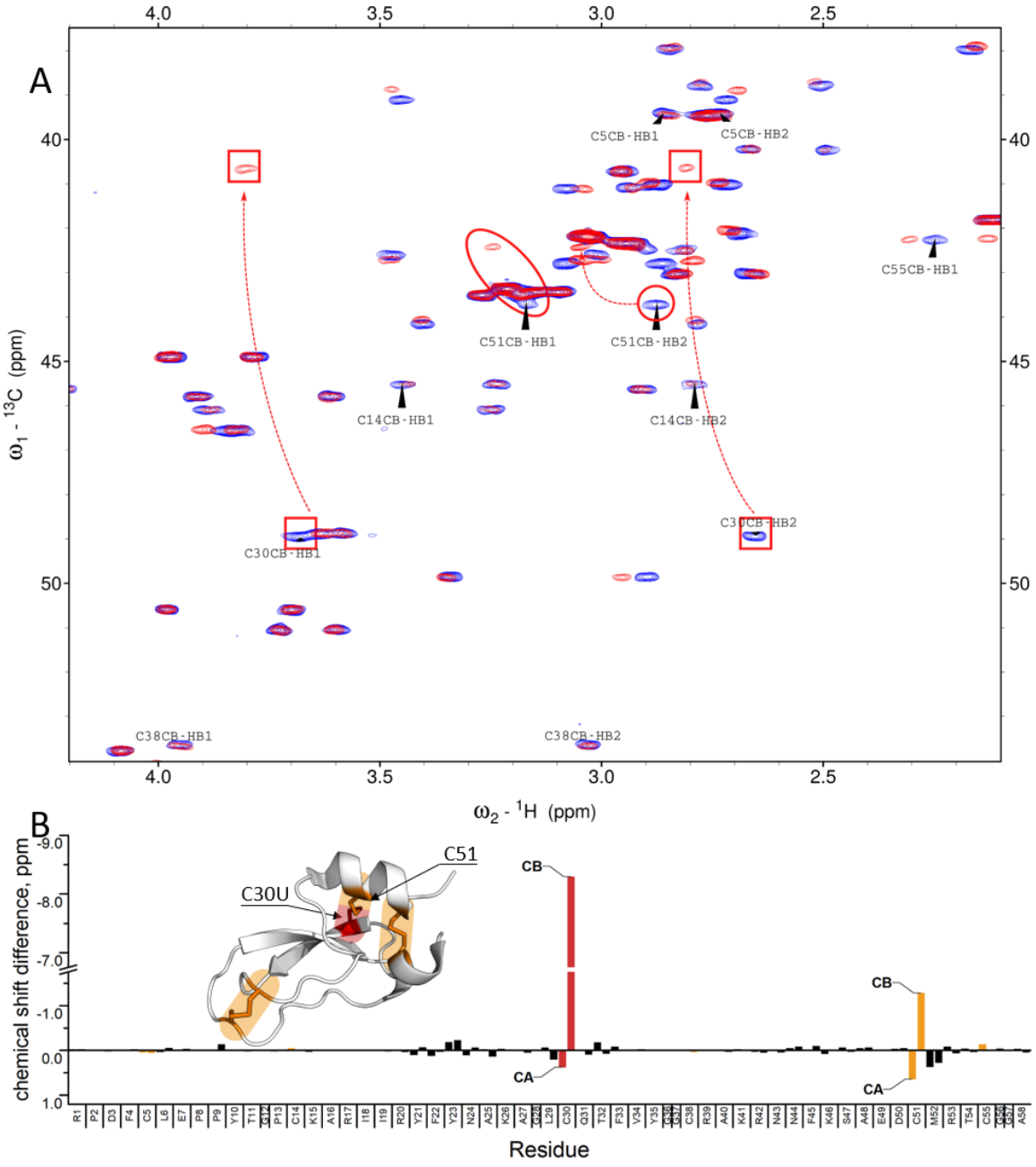

Figure S21. Chemical shift perturbations induced by Se in C30U BPTI.

A. Overlaid ^{1}H-^{13}C HSQC spectra of wt (blue) and C30U BPTI (red). Squares show the displacements of Hβ1/2-Cβ peaks of U30, ellipses display Hβ1/2-Cβ peak of the opposite C51 residue. B. Chemical shift difference plot of assigned carbon atoms in wt and C30U BPTI. Delta values derived for U30 are coloured red, values for other cysteines are coloured yellow.

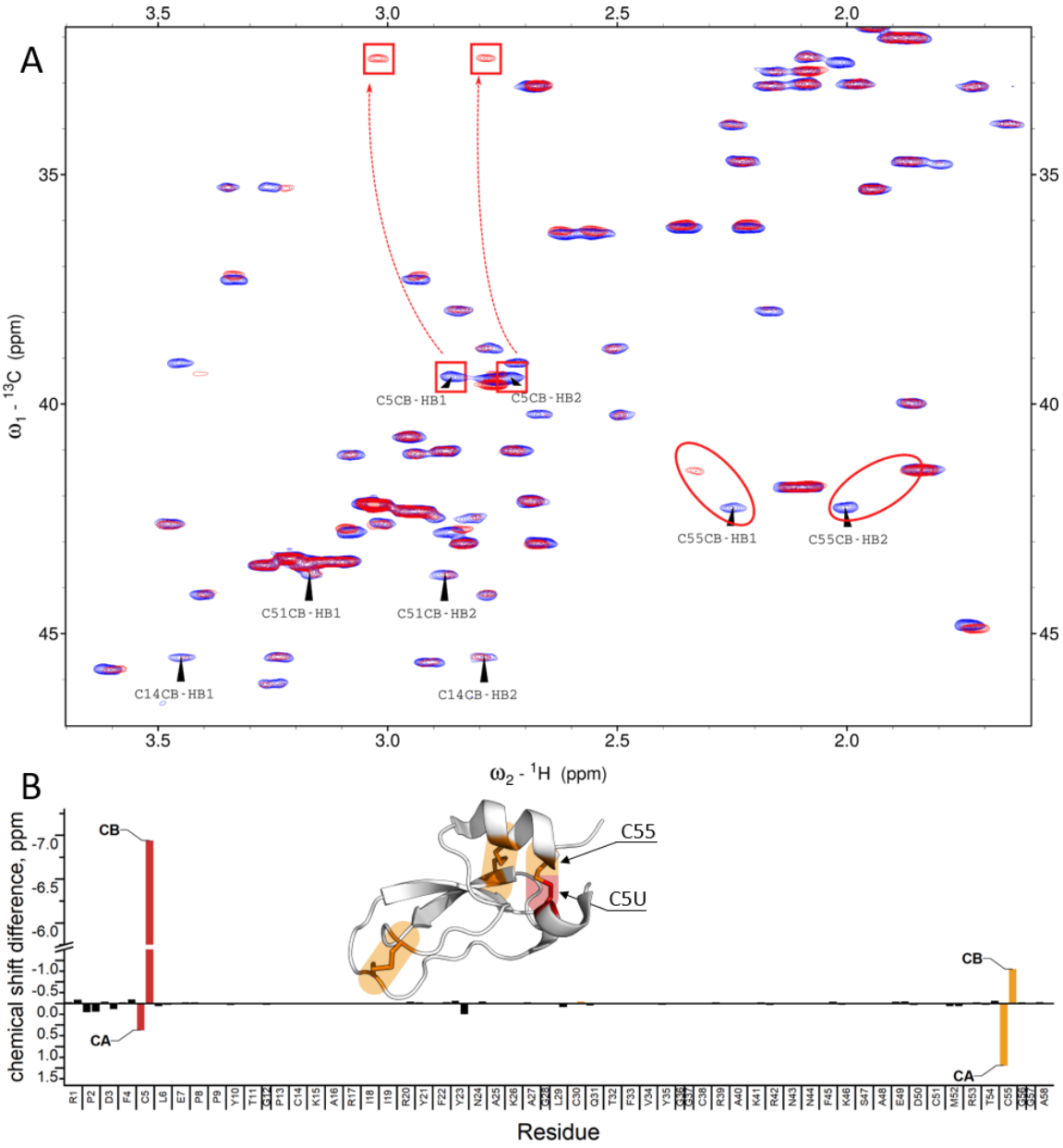

Figure S22. Chemical shift perturbations induced by Se in C5U BPTI.

A. Overlaid ^{1}H-^{13}C HSQC spectra of wt (blue) and C5U BPTI (red). Squares show the displacements of Hβ1/2-Cβ peaks of U5, ellipses display Hβ1/2-Cβ peak of the opposite C55 residue. B. Chemical shift difference plot of assigned carbon atoms in wt and C5U BPTI. Delta values derived for U5 are coloured red, values for other cysteines are coloured yellow.

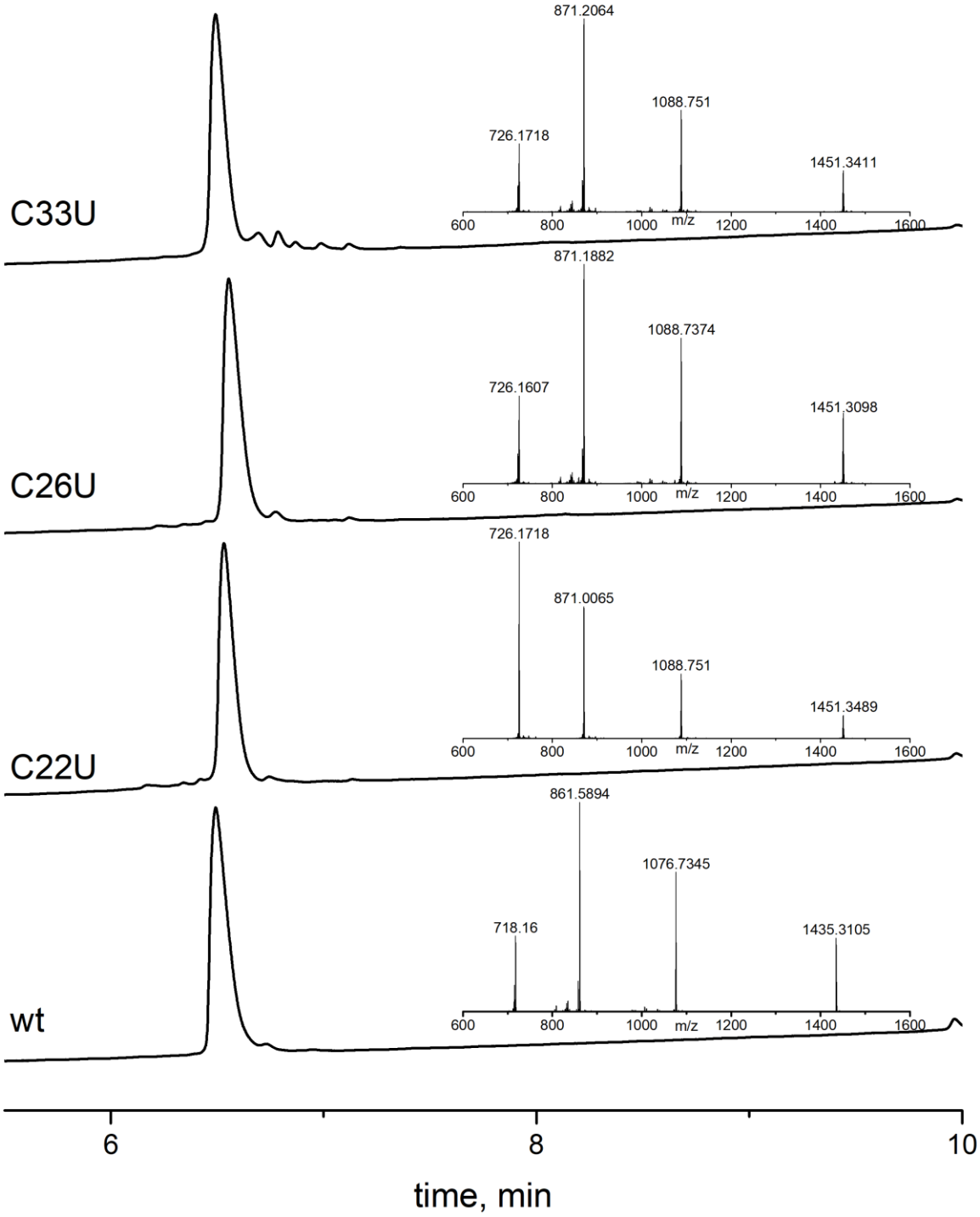

Figure S23. LC-MS analysis of purified tEv3 (17-56) variants.

Profiles of tEv3 (17-56) C33U, C26U, and C22U, in comparison to that of wild-type (wt) tEv3 (17-56).

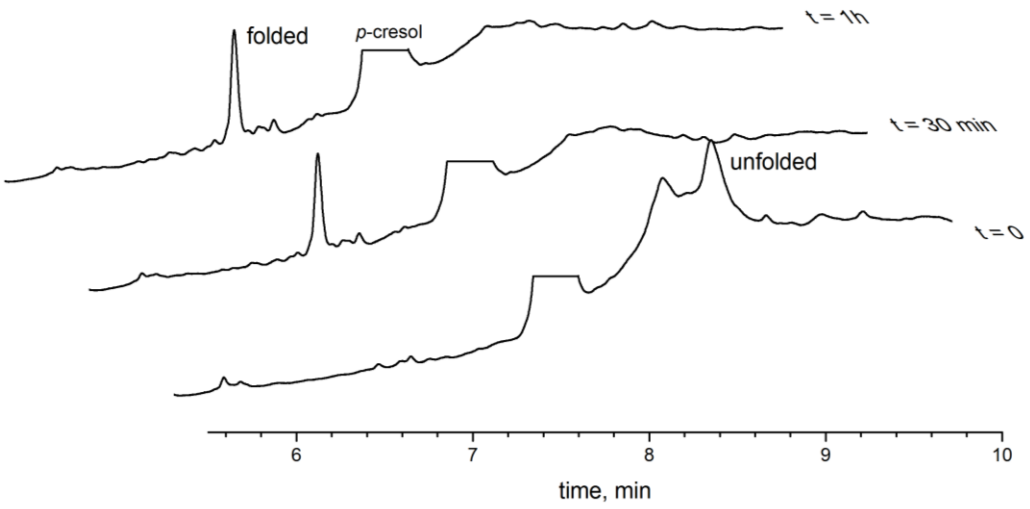

Figure S24. Folding kinetics of C26U tEv3 (17-56).

HPLC chromatograms of folding progression of C26U tEv3 (17-56) recorded at different time points during folding.

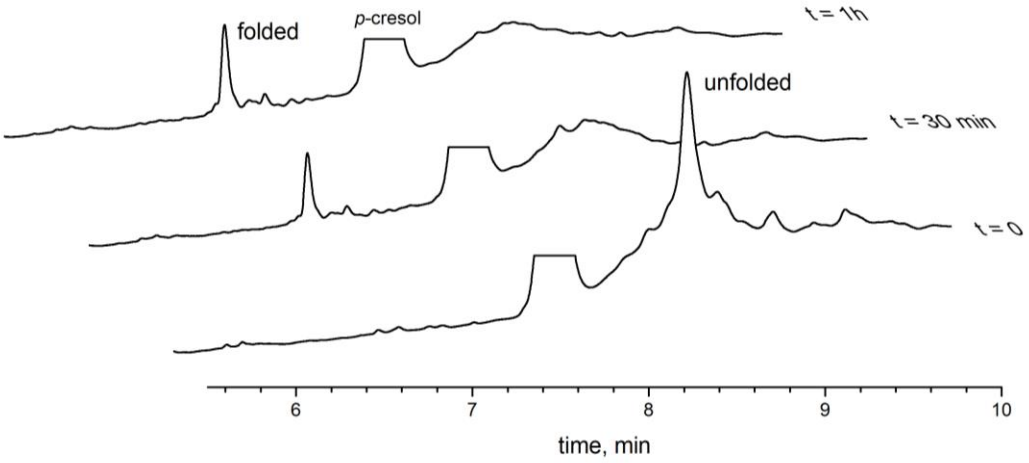

Figure S25. Folding kinetics of C33U tEv3 (17-56).

HPLC chromatograms of folding progression of C33U tEv3 (17-56) recorded at different time points during folding.

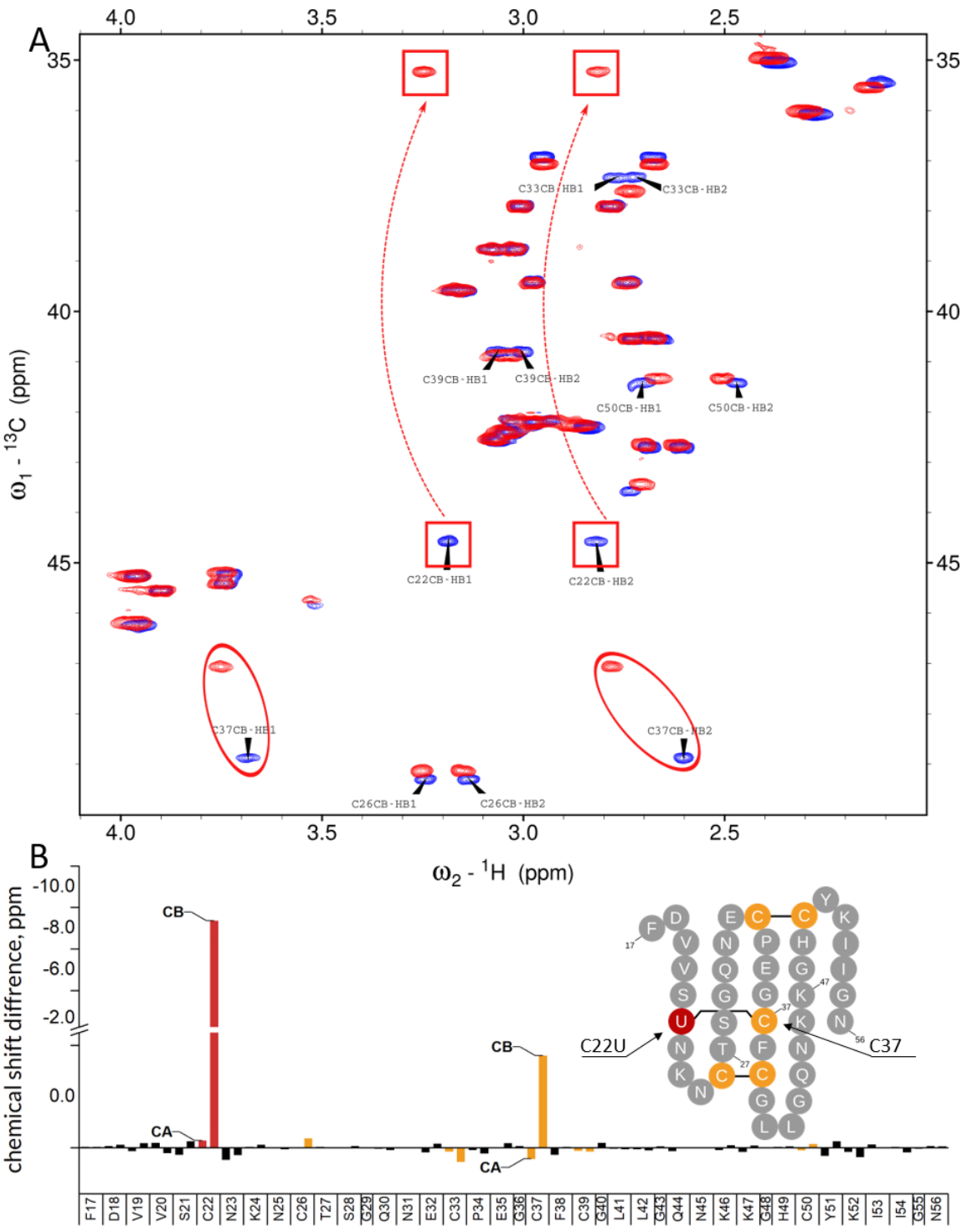

Figure S26. Chemical shift perturbations induced by Se in C22U tEv3 (17-56).

A. Overlaid ^{1}H-^{13}C HSQC spectra of wt (blue) and C22U tEv3 (17-56) (red). Squares show the displacements of Hβ1/2-Cβ peaks of U22, ellipses display Hβ1/2-Cβ peak of the opposite C37 residue. B. Chemical shift difference plot of assigned carbon atoms in wt and C22U tEv3 (17-56). Delta values derived for U22 are coloured red, values for other cysteines are coloured yellow.

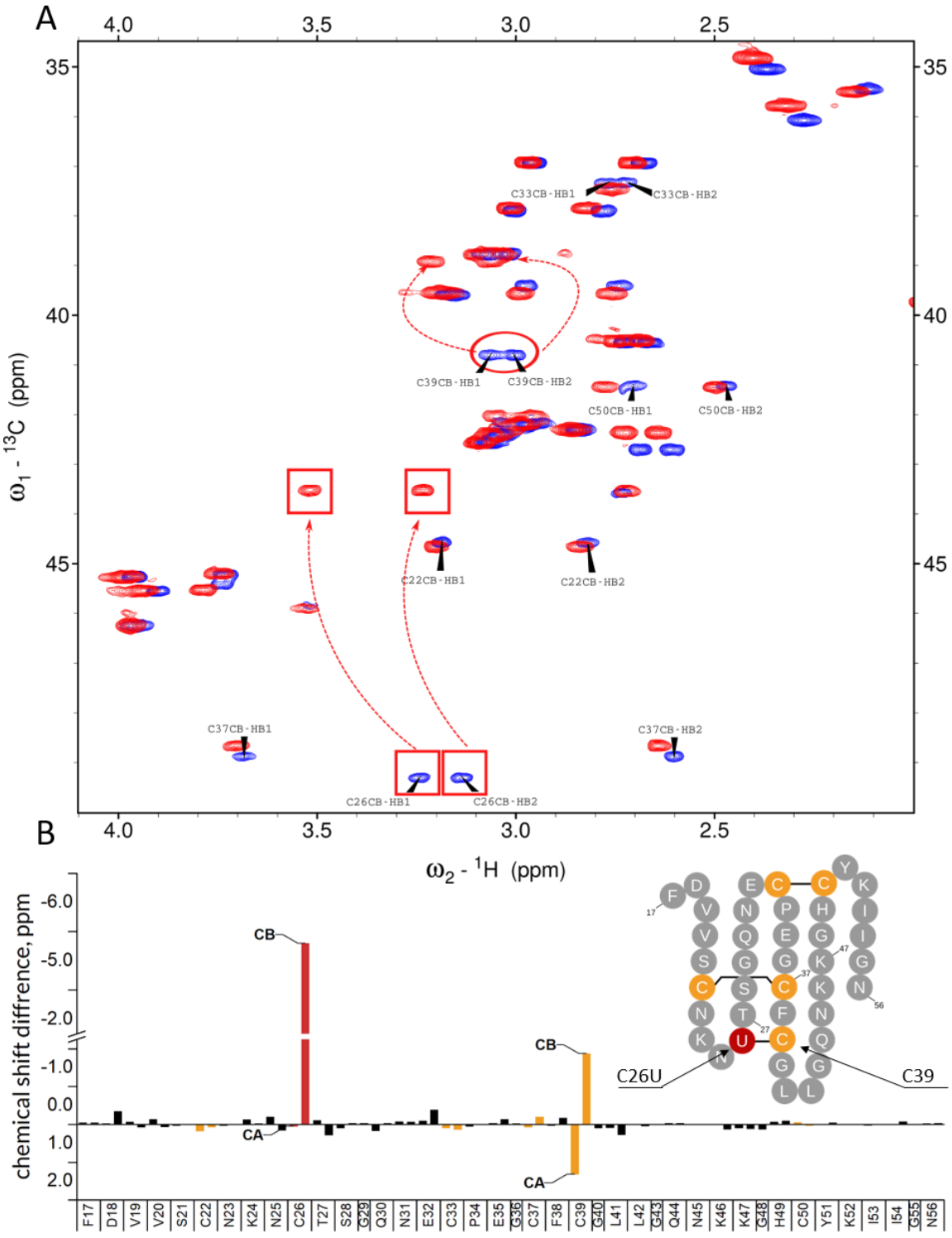

Figure S27. Chemical shift perturbations induced by Se in C26U tEv3 (17-56).

A. Overlaid ^{1}H-^{13}C HSQC spectra of wt (blue) and C26U tEv3 (17-56) (red). Squares show the displacements of Hβ1/2-Cβ peaks of U26, ellipses display Hβ1/2-Cβ peak of the opposite C39 residue. B. Chemical shift difference plot of assigned carbon atoms in wt and C22U tEv3 (17-56). Delta values derived for U22 are coloured red, values for other cysteines are coloured yellow.

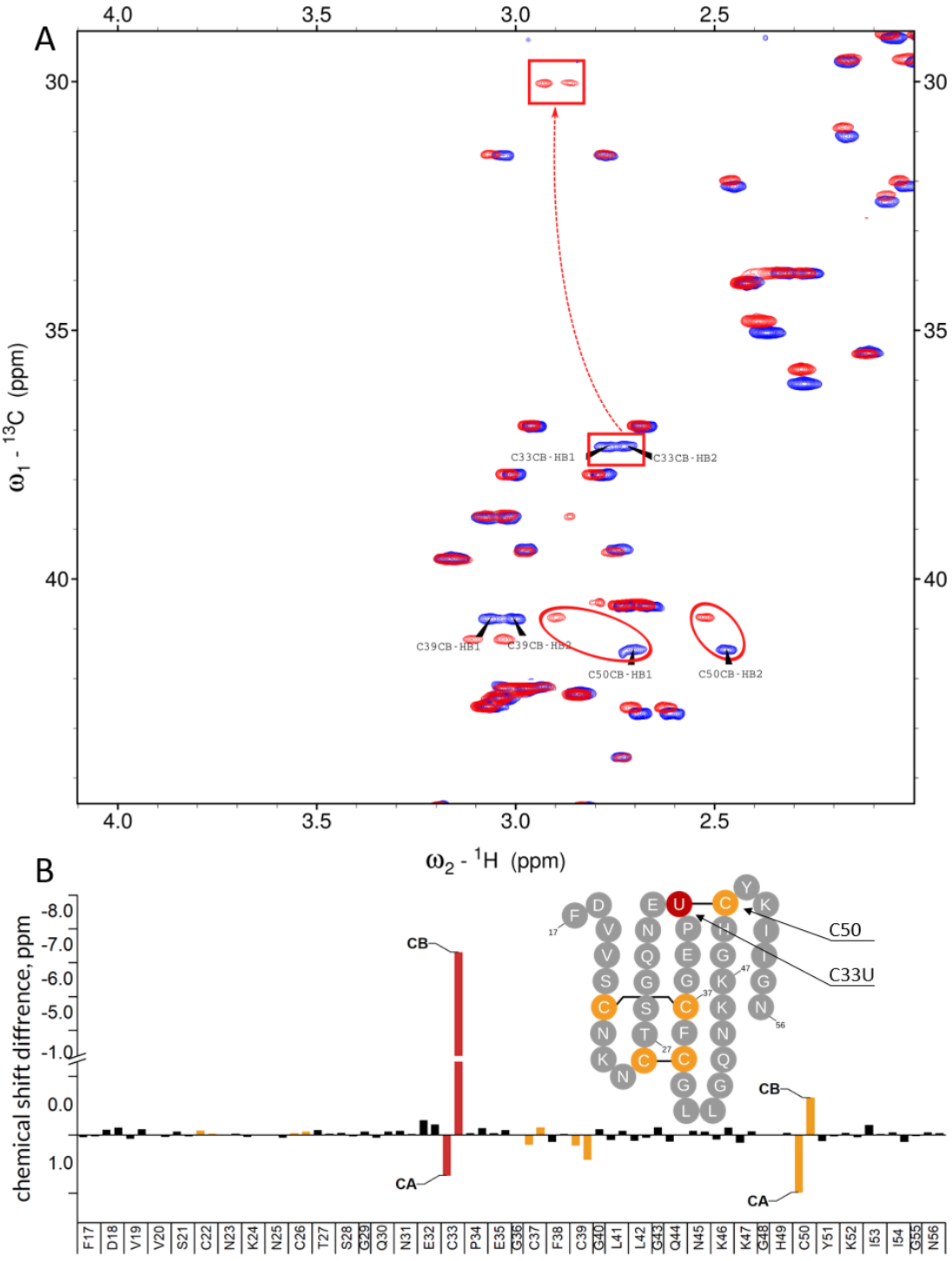

Figure S28. Chemical shift perturbations induced by Se in C33U tEv3 (17-56).

A. Overlaid ^{1}H-^{13}C HSQC spectra of wt (blue) and C33U tEv3 (17-56) (red). Squares show the displacements of Hβ1/2-Cβ peaks of U33, ellipses display Hβ1/2-Cβ peak of the opposite C50residue. B. Chemical shift difference plot of assigned carbon atoms in wt and C22U tEv3 (17-56). Delta values derived for U22 are coloured red, values for other cysteines are coloured yellow.

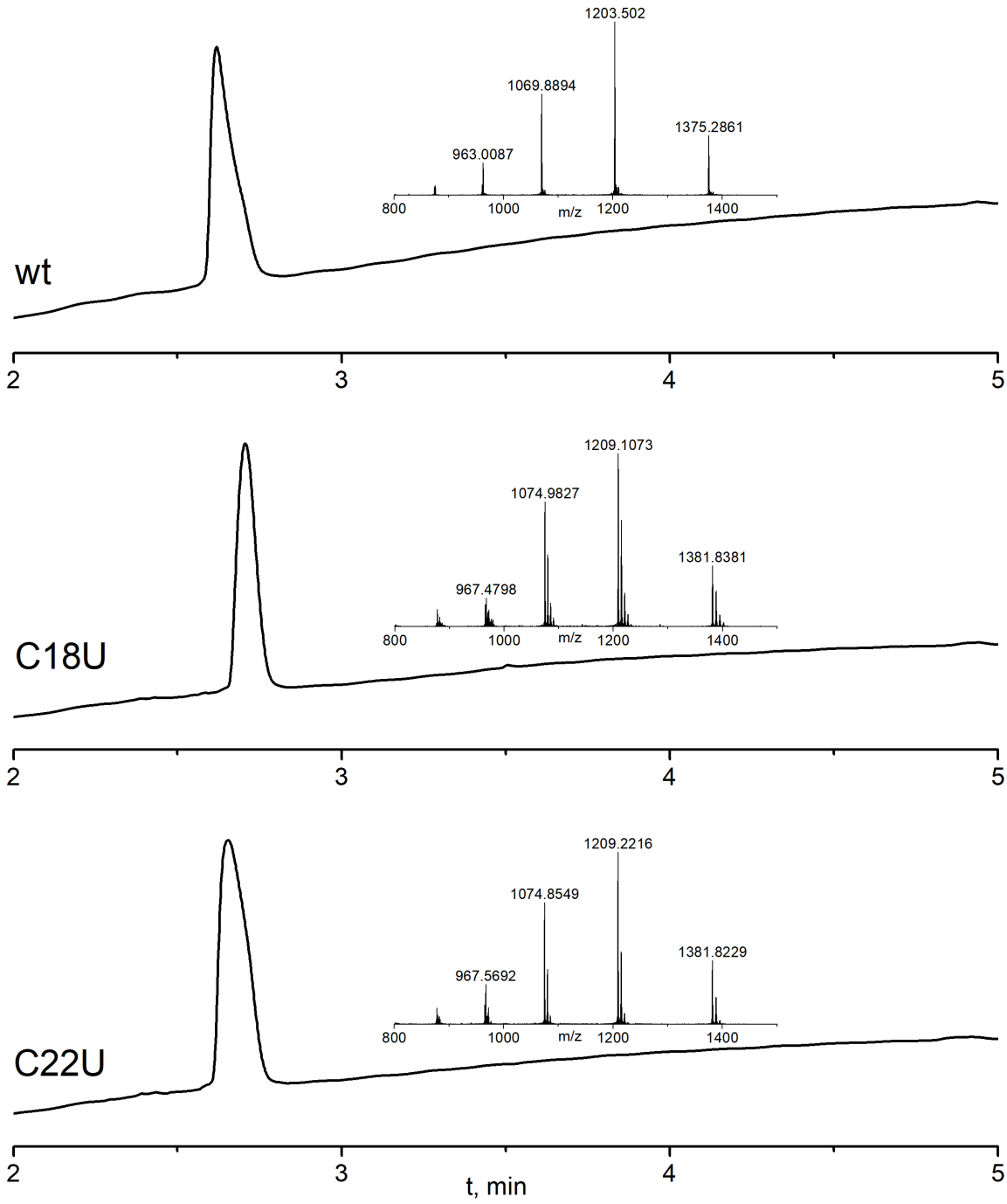

Figure S29. LC-MS analysis of purified BSAP1 variants.
Profiles of BSAP1 C18U and C22U in comparison to that of wild-type (wt) BSAP1.

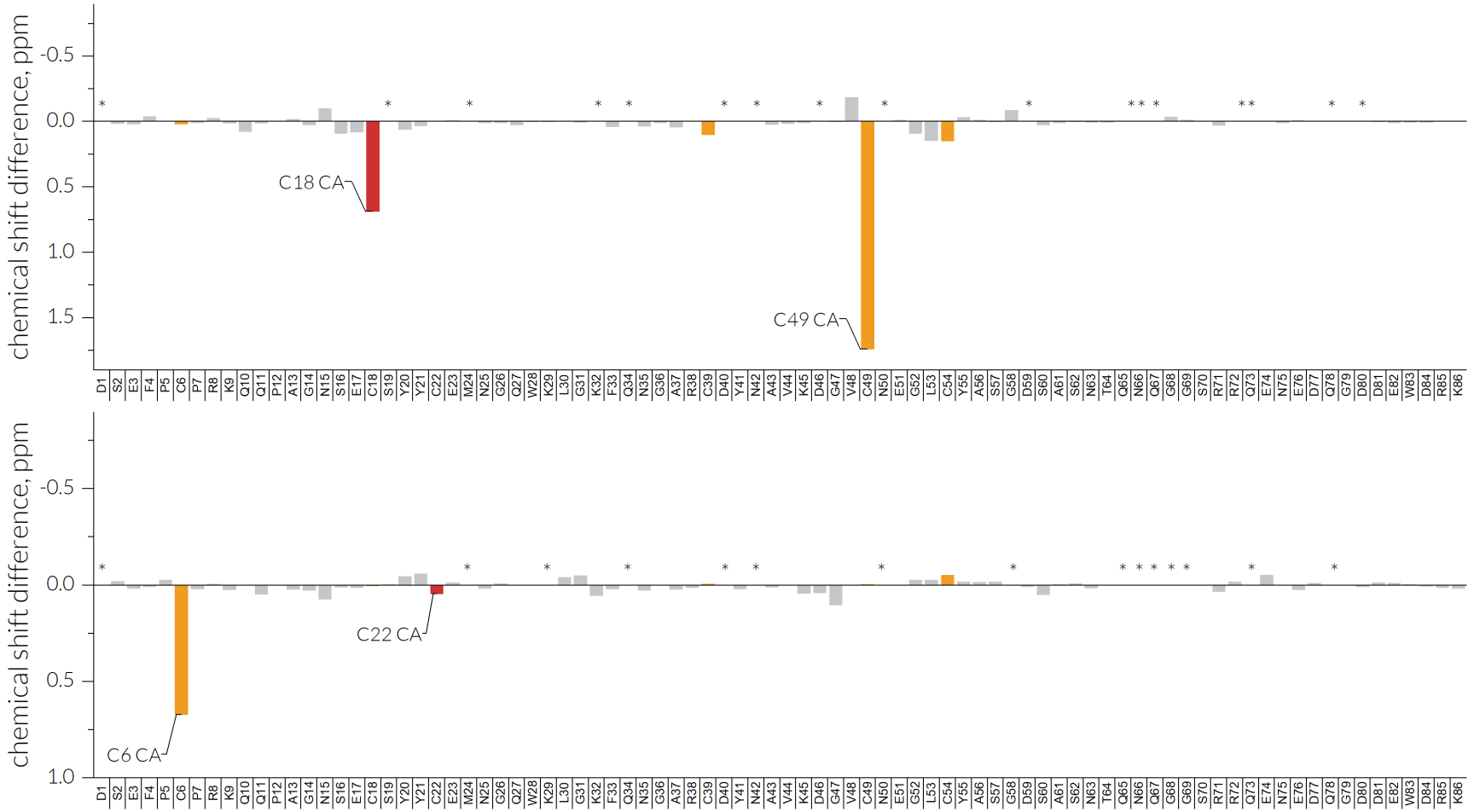

Figure S30. Chemical shift perturbations induced by Se in C18U and C22U BSAP1.

Chemical shift difference plot of assigned Cα carbon atoms between wt and C18U (top) and between wt and C22U (bottom) BSAP1. Delta values derived for selenocysteines are coloured red, values for other cysteines are coloured yellow; missing peaks are designated by *

Table S1. Sequences of synthetic peptides and proteins

Compound	Sequence
Arg-vasopressin (Uniprot: p01185, amino acids 20-28)	
WT	H_2N-Cys-Tyr-Phe-Gln-Asn-Cys-Pro-Arg-Gly-$CONH_2$
C1U	H_2N-**Sec**-Tyr-Phe-Gln-Asn-Cys-Pro-Arg-Gly-$CONH_2$
C6U	H_2N-Cys-Tyr-Phe-Gln-Asn-**Sec**-Pro-Arg-Gly-$CONH_2$
C1U/C6U	H_2N-**Sec**-Tyr-Phe-Gln-Asn-**Sec**-Pro-Arg-Gly-$CONH_2$
Kalata B1 (Uniprot: p56254, amino acids 89-117) prior to internal cyclisation	
WT	H_2N-Cys-Thr-Cys-Ser-Trp-Pro-Val-Cys-Thr-Arg-Asn-Gly-Leu-Pro-Val-Cys-Gly-Glu-Thr-Cys-Val-Gly-Gly-Thr-Cys-Asn-Thr-Pro-Gly-MPAL
C5U	H_2N-Cys-Thr-Cys-Ser-Trp-Pro-Val-**Sec**-Thr-Arg-Asn-Gly-Leu-Pro-Val-Cys-Gly-Glu-Thr-Cys-Val-Gly-Gly-Thr-Cys-Asn-Thr-Pro-Gly-MPAL
C22U	H_2N-Cys-Thr-Cys-Ser-Trp-Pro-Val-Cys-Thr-Arg-Asn-Gly-Leu-Pro-Val-Cys-Gly-Glu-Thr-Cys-Val-Gly-Gly-Thr-**Sec**-Asn-Thr-Pro-Gly-MPAL
C27U	H_2N-**Sec**-Thr-Cys-Ser-Trp-Pro-Val-Cys-Thr-Arg-Asn-Gly-Leu-Pro-Val-Cys-Gly-Glu-Thr-Cys-Val-Gly-Gly-Thr-Cys-Asn-Thr-Pro-Gly-MPAL
C29U	H_2N-Cys-Thr-**Sec**-Ser-Trp-Pro-Val-Cys-Thr-Arg-Asn-Gly-Leu-Pro-Val-Cys-Gly-Glu-Thr-Cys-Val-Gly-Gly-Thr-Cys-Asn-Thr-Pro-Gly-MPAL
μ-Conotoxin KIIIA (Uniprot: p0C195, amino acids 1-16)	
WT	H_2N-Cys-Cys-Asn-Cys-Ser-Ser-Lys-Trp-Cys-Arg-Asp-His-Ser-Arg-Cys-Cys-$CONH_2$
C1U	H_2N-**Sec**-Cys-Asn-Cys-Ser-Ser-Lys-Trp-Cys-Arg-Asp-His-Ser-Arg-Cys-Cys-$CONH_2$
C2U	H_2N-Cys-**Sec**-Asn-Cys-Ser-Ser-Lys-Trp-Cys-Arg-Asp-His-Ser-Arg-Cys-Cys-$CONH_2$
C4U	H_2N-Cys-Cys-Asn-**Sec**-Ser-Ser-Lys-Trp-Cys-Arg-Asp-His-Ser-Arg-Cys-Cys-$CONH_2$
BPTI (Uniprot: p00974, amino acids 36-93)	
C-terminus	H_2N-Cys-Arg-Ala-Lys-Arg-Asn-Asn-Phe-Lys-Ser-Ala-Glu-Asp-Cys-Met-Arg-Thr-Cys-Gly-Gly-Ala-COOH
WT N-terminus	H_2N-Arg-Pro-Asp-Phe-Cys-Leu-Glu-Pro-Pro-Tyr-Thr-Gly-Pro-Cys-Lys-Ala-Arg-Ile-Ile-Arg-Tyr-Phe-Tyr-Asn-Ala-Lys-Ala-Gly-Leu-Cys-Gln-Thr-Phe-Val-Tyr-Gly-Gly-MPAL
C5U N-terminus	H_2N-Arg-Pro-Asp-Phe-**Sec**-Leu-Glu-Pro-Pro-Tyr-Thr-Gly-Pro-Cys-Lys-Ala-Arg-Ile-Ile-Arg-Tyr-Phe-Tyr-Asn-Ala-Lys-Ala-Gly-Leu-Cys-Gln-Thr-Phe-Val-Tyr-Gly-Gly-MPAL
C14U N-terminus	H_2N-Arg-Pro-Asp-Phe-Cys-Leu-Glu-Pro-Pro-Tyr-Thr-Gly-Pro-**Sec**-Lys-Ala-Arg-Ile-Ile-Arg-Tyr-Phe-Tyr-Asn-Ala-Lys-Ala-Gly-Leu-Cys-Gln-Thr-Phe-Val-Tyr-Gly-Gly-MPAL

C30U N-terminus	H_2N-Arg-Pro-Asp-Phe-Cys-Leu-Glu-Pro-Pro-Tyr-Thr-Gly-Pro-Cys-Lys-Ala-Arg-Ile-Ile-Arg-Tyr-Phe-Tyr-Asn-Ala-Lys-Ala-Gly-Leu-**Sec**-Gln-Thr-Phe-Val-Tyr-Gly-Gly-MPAL
Truncated Evasin-3 (Uniprot: p0c8e8, amino acids 17-56)	
WT	H_2N-Phe-Asp-Val-Val-Ser-Cys-Asn-Lys-Asn-Cys-Thr-Ser-Gly-Gln-Asn-Glu-Cys-Pro-Glu-Gly-Cys-Phe-Cys-Gly-Leu-Leu-Gly-Gln-Asn-Lys-Lys-Gly-His-Cys-Tyr-Lys-Ile-Ile-Gly-Asn-COOH
C22U	H_2N-Phe-Asp-Val-Val-Ser-**Sec**-Asn-Lys-Asn-Cys-Thr-Ser-Gly-Gln-Asn-Glu-Cys-Pro-Glu-Gly-Cys-Phe-Cys-Gly-Leu-Leu-Gly-Gln-Asn-Lys-Lys-Gly-His-Cys-Tyr-Lys-Ile-Ile-Gly-Asn-COOH
C26U	H_2N-Phe-Asp-Val-Val-Ser-Cys-Asn-Lys-Asn-**Sec**-Thr-Ser-Gly-Gln-Asn-Glu-Cys-Pro-Glu-Gly-Cys-Phe-Cys-Gly-Leu-Leu-Gly-Gln-Asn-Lys-Lys-Gly-His-Cys-Tyr-Lys-Ile-Ile-Gly-Asn-COOH
C33U	H_2N-Phe-Asp-Val-Val-Ser-Cys-Asn-Lys-Asn-Cys-Thr-Ser-Gly-Gln-Asn-Glu-**Sec**-Pro-Glu-Gly-Cys-Phe-Cys-Gly-Leu-Leu-Gly-Gln-Asn-Lys-Lys-Gly-His-Cys-Tyr-Lys-Ile-Ile-Gly-Asn-COOH

Mutations are designated in red.

Table S2. Sequences of BSAP1 variants genes

Variant	ORF sequence
WT	catatgggcCACCACCACCACCACCACggtagcctgcaagatagcgaggttaatcaagaa M G H H H H H H G S L Q D S E V N Q E gcgaagccggaagtgaagccggaagtgaagccggaaacccacatcaacctgaaggtgagc A K P E V K P E V K P E T H I N L K V S gatggcagcagcgaaatcttctttaagattaagaaaaccacccgctgcgtcgtctgatg D G S S E I F F K I K K T T P L R R L M gaggcgttcgcgaagcgtcagggcaaagaaatggacagcctgcgttttctgtacgatggt E A F A K R Q G K E M D S L R F L Y D G atccgtattcaggcggaccaagcgccggaggacctggatatggaagacaacgatatcatt I R I Q A D Q A P E D L D M E D N D I I gaggcgcaccgtgaacaaattggtggcgatagcgagtttccgtgcccgcgtaagcagcaa E A H R E Q I G G D S E F P C P R K Q Q ccggcgggcaacagcgagtgcagctactattgcgaaatgaacggccagtggaagctgggc P A G N S E C S Y Y C E M N G Q W K L G aaatttcaaaacggtgcgcgttgcgactacaacgcggtgaaagatggcgtttgcaacgaa K F Q N G A R C D Y N A V K D G V C N E ggtctgtgctatgcgagcggtgacagcgcgagcaacacccagaaccagggtggcagccgc G L C Y A S G D S A S N T Q N Q G G S R cgtcaagaaaacgaagaccagggtgatgatgaatgggaccgcaaataaagctt R Q E N E D Q G D D E W D R K -
C22U	catatgggcCACCACCACCACCACCACggtagcctgcaagatagcgaggttaatcaagaa M G H H H H H H G S L Q D S E V N Q E gcgaagccggaagtgaagccggaagtgaagccggaaacccacatcaacctgaaggtgagc A K P E V K P E V K P E T H I N L K V S gatggcagcagcgaaatcttctttaagattaagaaaaccacccgctgcgtcgtctgatg D G S S E I F F K I K K T T P L R R L M gaggcgttcgcgaagcgtcagggcaaagaaatggacagcctgcgttttctgtacgatggt E A F A K R Q G K E M D S L R F L Y D G atccgtattcaggcggaccaagcgccggaggacctggatatggaagacaacgatatcatt I R I Q A D Q A P E D L D M E D N D I I gaggcgcaccgtgaacaaattggtggcgatagcgagtttccgtgcccgcgtaagcagcaa E A H R E Q I G G D S E F P C P R K Q Q ccggcgggcaacagcgagtgcagctactat**tag**gaaatgaacggccagtggaagctgggc P A G N S E C S Y Y **U** E M N G Q W K L G aaatttcaaaacggtgcgcgttgcgactacaacgcggtgaaagatggcgtttgcaacgaa K F Q N G A R C D Y N A V K D G V C N E ggtctgtgctatgcgagcggtgacagcgcgagcaacacccagaaccagggtggcagccgc G L C Y A S G D S A S N T Q N Q G G S R cgtcaagaaaacgaagaccagggtgatgatgaatgggaccgcaaataaagctt R Q E N E D Q G D D E W D R K -
C18U	catatgggcCACCACCACCACCACCACggtagcctgcaagatagcgaggttaatcaagaa M G H H H H H H G S L Q D S E V N Q E gcgaagccggaagtgaagccggaagtgaagccggaaacccacatcaacctgaaggtgagc A K P E V K P E V K P E T H I N L K V S gatggcagcagcgaaatcttctttaagattaagaaaaccacccgctgcgtcgtctgatg D G S S E I F F K I K K T T P L R R L M gaggcgttcgcgaagcgtcagggcaaagaaatggacagcctgcgttttctgtacgatggt E A F A K R Q G K E M D S L R F L Y D G atccgtattcaggcggaccaagcgccggaggacctggatatggaagacaacgatatcatt I R I Q A D Q A P E D L D M E D N D I I gaggcgcaccgtgaacaaattggtggcgatagcgagtttccgtgcccgcgtaagcagcaa E A H R E Q I G G D S E F P C P R K Q Q

	ccggcgggcaacagcgag**tag**agctactattgcgaaatgaacggccagtggaagctgggc P A G N S E **U** S Y Y C E M N G Q W K L G aaatttcaaaacggtgcgcgttgcgactacaacgcggtgaaagatggcgtttgcaacgaa K F Q N G A R C D Y N A V K D G V C N E ggtctgtgctatgcgagcggtgacagcgcgagcaacacccagaaccagggtggcagccgc G L C Y A S G D S A S N T Q N Q G G S R cgtcaagaaaacgaagaccagggtgatgatgaatgggaccgcaaataaagctt R Q E N E D Q G D D E W D R K -

His tag is designated in blue, SUMO tag – green, mutations - in red.

Table S3. Summary table of calculated and observed by ESI-MS masses for all peptides and proteins.

Peptide/protein	Calculated monoisotopic mass in unfolded state, Da	Observed monoisotopic mass in unfolded state [M+H], Da	Calculated monoisotopic mass in oxidized state, Da	Observed monoisotopic mass in oxidized state [M+H], Da
Arg-vasopressin				
wt	1085.45	1086.49	1083.44	1084.44
C1U	1133.40	ND*	1131.38	1132.44
C6U	1133.40	ND*	1131.38	1132.45
C1U/C6U	1181.34	ND*	1179.33	1180.37
μ-conotoxin KIIIA				
wt	1888.68	1889.80	1882.63	1883.85
C1U	1936.63	1936.01	1930.58	1931.87
C2U	1936.63	1935.99	1930.58	1931.93
C4U	1936.63	1935.81	1930.58	1931.89
Kalata B1				
wt	3115.20**	3116.46**	2890.14	2891.34
C5U	3163.14**	3164.39**	2938.08	2939.31
C22U	3163.14**	3163.33**	2938.08	2938.30
C27U	3163.14**	3163.47**	2938.08	2939.24
C29U	3163.14**	3162.37**	2938.08	2939.25
BPTI				
wt	6513.08	6514.30	6507.08	6508.06
C5U	6561.03	6560.36	6554.98	6556.12
C14U	6561.03	6559.04	6554.98	6555.21
C30U	6561.03	6559.97	6554.98	6556.22
tEv3 (17-56)				
wt	4306.91	4308.11	4300.86	4301.92
C22U	4354.86	4352.98	4348.81	4348.98
C26U	4354.86	4352.88	4348.81	4349.92
C33U	4354.86	4353.89	4348.81	4348.97
BSAP1				
wt	9618.09		9612.05	9613.09
C18U	9666.04	ND*	9659.99	9660.76
C22U	9666.04	ND*	9659.99	9661.45

* reduced forms of Sec-mutants in Arg-vasopressin or BSAP-1 were not observed. ** - mass corresponding to linear Kalata B1 prior to cyclization and oxidative folding.

Table S4. Summary table of chemical shift differences for Cα/Cβ cysteine atoms.

Compound		Cysteines Cα/Cβ chemical shift difference, ppm					
		C1	C2	C4	C9	C15	C16
KIIIA [C1-C15, C2-C9, C4-C16][6]	C1U	0.379/-7.952	0.216/-0.097	0.007/-0.044	0.094/0.048	**0.108/-0.781**	0.147/-0.394
	C2U	0.112/-0.096	-0.166/-7.102	0.056/0.252	**1.194/-0.676**	0.283/-0.045	0.0440.060
	C4U	-0.003/0.053	-0.020/-0.053	0.648/-7.820	0.012/-0.015	-0.058/0.050	**1.376/-1.044**
		C5	C13	C17	C22	C27	C29
Kalata B1 [C5-C22, C13-C27, C17-C29][7]	C5U	0.782/-7.054	0.057/0.053	0.480/-0.313	**0.663/-0.771**	-0.046/-0.264	0.264/0.591
	C22U	**1.149/-0.819**	0.032/0.210	-0.164/0.072	0.228/-6.854	0.034/-0.619	0.057/0.073
	C27U	0.124/-0.084	**0.456/-0.813**	-0.083/0.168	0.109/0.059	0.242/-7.882	-0.113/-0.104
	C29U	-0.209/-0.016	0.029/0.001	**0.683/-0.394**	0.003/-0.165	0.003/0.001	0.763/-8.422
		C5	C14	C30	C38	C51	C55
BPTI [C5-C55, C14-C38, C30-C51][8]	C5U	0.624/-6.941	0.017/0.000	-0.010/-0.046	-0.006/0.012	0.019/0.006	**1.441/-0.799**
	C14U	-0.001/-0.002	-0.044/-7.305	0.003/-0.006	**0.602/-1.444**	-0.004/0.021	-0.027/0.011
	C30U	0.042/0.053	-0.047/-0.014	0.373/-8.296	0.006/0.036	**0.642/-1.282**	-0.135/-0.001
		C22	C26	C33	C37	C39	C50
tEv3(17-56) [C22-C37, C26-C39, C33-C50]**	C22U	-0.137/-9.348	-0.006/-0.183	0.067/0.268	**0.219/-1.803**	0.050/0.072	0.046/-0.073
	C26U	0.174/0.076	0.050/-5.799	0.090/0.134	0.072/-0.203	**1.314/-1.876**	-0.048/0.034
	C33U	-0.070-0.015	-0.023/-0.051	0.690/-7.308	0.167/-0.127	0.180/0.425	**0.986/-0.636**
		C6	C18	C22	C39	C49	C54
BSAP1 [C6-C22, C18-C22, C39-C54]**	C18U	0.02/ 0.039	0.687/*	-0.002/ -0.013	0.102/ 0.459	**1.738/***	0.148/*
	C22U	**0.672/***	0.003/ -0.028	0.045/*	-0.005/ 0.037	-0.003/ -0.069	-0.052/ -0.015

SecScan disulfide bonds (red to yellow) for each Sec mutant follow from the experimental chemical shift differences in Cys. The pair of Δδ Cα and Δδ Cβ values that are perturbed the most (yellow) indicates the presence of a mixed S-Se covalent bond between Cys and the introduced single Sec residue (red). Disulfide bonds are listed in square brackets given in the left column. * missing data; ** this manuscript

References

1 N. L. Daly, S. Love, P. F. Alewood and D. J. Craik, *Biochemistry*, 1999, **38**, 10606–10614.

2 W. Lu, M. A. Starovasnik and S. B. Kent, *FEBS Lett.*, 1998, **429**, 31–35.

3 M. Takeda, Y. Miyanoiri, T. Terauchi and M. Kainosho, *J. Biomol. NMR*, 2016, **66**, 37–53.

4 T. L. Hwang and A. J. Shaka, *J. Magn. Reson. Ser. A*, 1995, **112**, 275–279.

5 L. Castañar, J. Saurí, R. T. Williamson, A. Virgili and T. Parella, *Angew. Chem. Int. Ed. Engl.*, 2014, **53**, 8379–82.

6 K. K. Khoo, K. Gupta, B. R. Green, M.-M. Zhang, M. Watkins, B. M. Olivera, P. Balaram, D. Yoshikami, G. Bulaj and R. S. Norton, *Biochemistry*, 2012, **51**, 9826–9835.

7 O. Saether, D. J. Craik, I. D. Campbell, K. Sletten, J. Juul and D. G. Norman, *Biochemistry*, 1995, **34**, 4147–4158.

8 P. Ascenzi, A. Bocedi, M. Bolognesi, A. Spallarossa, M. Coletta, R. Cristofaro and E. Menegatti, *Curr. Protein Pept. Sci.*, 2003, **4**, 231–251.